

A Visuospatial Planning Task Coupled with Eye-Tracker and Electroencephalogram Systems

Marcos Domic-Siede¹, Martín Irani², Joaquín Valdés³, María Rodríguez^{4,5}, Brice Follet^{3,6}, Marcela Perrone-Bertolotti^{7,8}, Tomás Ossandón³

¹Laboratorio de Neurociencia Cognitiva, Escuela de Psicología, Universidad Católica del Norte ²Department of Psychology, University of Illinois Urbana-Champaign ³Neurodynamics of Cognition Laboratory, Departamento de Psiquiatría, Pontificia Universidad Católica de Chile ⁴Instituto de Ciencias de la Salud, Universidad de O'Higgins ⁵Instituto de Ciencias de la Ingeniería, Universidad de O'Higgins ⁶Department of Psychiatry, University Hospital of Saint-Etienne ⁷Univ. Grenoble Alpes, Univ. Savoie Mont Blanc, CNRS, LPNC ⁸Institut Universitaire de France (IUF)

Corresponding Authors

Marcos Domic-Siede

mdomic@ucn.cl

Marcela Perrone-Bertolotti

marcela.perrone-bertolotti@univ-grenoble-alpe

Tomás Ossandón

tossandonv@uc.cl

Citation

Domic-Siede, M., Irani, M., Valdés, J., Rodríguez, M., Follet, B., Perrone-Bertolotti, M., Ossandón, T. A. Visuospatial Planning Task Coupled with Eye-Tracker and Electroencephalogram Systems. *J. Vis. Exp.* (193), e64622, doi:10.3791/64622 (2023).

Date Published

March 3, 2023

DOI

10.3791/64622

URL

jove.com/video/64622

Abstract

The planning process, characterized by the capability to formulate an organized plan to reach a goal, is essential for human goal-directed behavior. Since planning is compromised in several neuropsychiatric disorders, the implementation of proper clinical and experimental tests to examine planning is critical. Due to the nature of the deployment of planning, in which several cognitive domains participate, the assessment of planning and the design of behavioral paradigms coupled with neuroimaging methods are current challenges in cognitive neuroscience. A planning task was evaluated in combination with an electroencephalogram (EEG) system and eye movement recordings in 27 healthy adult participants. Planning can be separated into two stages: a mental planning stage in which a sequence of steps is internally represented and an execution stage in which motor action is used to achieve a previously planned goal. Our protocol included a planning task and a control task. The planning task involved solving 36 maze trials, each representing a zoo map. The task had four periods: i) planning, where the subjects were instructed to plan a path to visit the locations of four animals according to a set of rules; ii) maintenance, where the subjects had to retain the planned path in their working memory; iii) execution, where the subjects used eye movements to trace the previously planned path as indicated by the eye-tracker system; and iv) response, where the subjects reported the order of the visited animals. The control task had a similar structure, but the cognitive planning component was removed by modifying the task goal. The spatial and temporal patterns of the EEG revealed that planning induces a gradual and lasting rise in frontal-midline theta activity (FM θ) over time. The source of this activity was identified within the prefrontal cortex by source analyses. Our results suggested that

the experimental paradigm combining EEG and eye-tracker systems was optimal for evaluating cognitive planning.

Introduction

During the past 10 years, extensive research has been conducted to examine the role of oscillatory neural dynamics on both cognition and behavior. These studies have established that frequency-specific interactions between specialized and widespread cortical regions play a crucial role in cognition and cognitive control^{1,2,3}. This approach highlights the rhythmic nature of brain activity, which helps coordinate large-scale cortical dynamics and underpins cognitive processing and goal-directed behavior^{4,5}. There is substantial evidence showing that rhythmic oscillations in the brain are involved in various cognitive processes, including perception⁶, attention^{7,8,9}, decision-making¹⁰, memory reactivation¹¹, working memory¹², and cognitive control¹³. Different oscillatory mechanisms have been proposed to guide goal-directed behavior, with transient large-scale frequency-specific networks providing a framework for cognitive processing^{1,14,15}. For example, recent findings suggest that specific frequency bands in the brain may reflect a feedback mechanism that regulates spiking activity, providing a temporal reference frame to coordinate cortical excitability and spike timing for producing behavior^{16,17,18}. A review is provided by Helfrich and Knight¹⁹.

This body of evidence raises questions about how the prefrontal cortex (PFC) encodes planning task contexts and related behaviorally relevant rules. The PFC has long been thought to support cognitive control and goal-directed behavior through the oscillatory patterns of neural activity it generates, selectively biasing the neural activity in distant brain regions and controlling the flow of information in

large-scale neural networks²⁰. Additionally, it has been proposed that regions exhibiting local synchrony are more likely to participate in inter-regional activity^{21,22,23}. In particular, cortical theta-band (4-8 Hz) oscillations, as measured by scalp electroencephalogram (EEG), have been proposed as a potential mechanism for transmitting top-down control across broad networks¹³. Specifically, theta-band activity in humans reflects high-level cognitive processes, such as memory encoding and retrieval, working memory retention, novelty detection, decision-making, and top-down control^{12,24,25,26}.

Related to this, Cavanagh and Frank¹³ proposed two sequential mechanisms of control processes: the recognition of the need for control and the instantiation of control. The recognition of the need for control may be indicated by frontal midline theta (FM θ) activity originating from the medial prefrontal cortex (mPFC), which has been described in terms of event-related potential (ERP) components that reflect mPFC-related control processes in response to various situations, such as novel information^{27,28,29}, conflicting stimulus-response requirements³⁰, error feedback³¹, and error detection³². These ERP components, which reflect the need for increased cognitive control in the presence of novelty, conflict, punishment, or error, exhibit a common spectral signature in the theta band recorded at frontal midline electrodes^{26,27,33,34,35,36,37,38,39,40,41,42,43,44}.

The EEG responses of FM θ activity display a pattern of phase reset and power enhancement in the theta frequency band²⁶. Despite the limitations of the EEG

method in terms of its spatial resolution, various sources of evidence have been collected to demonstrate that FM θ activity is generated by the mid-cingulate cortex (MCC)¹³. These theta dynamics are believed to serve as temporal frameworks that regulate the neuronal processes of the mPFC, which are subsequently augmented in response to events requiring heightened control²⁶. This has been established through source analysis^{31,33,45,46,47}, concurrent EEG and functional magnetic resonance imaging (fMRI) recordings^{48,49}, and invasive EEG recordings in humans⁵⁰ and monkeys^{51,52,53}.

Based on these observations, the frontal midline theta is considered to serve as a universal mechanism, a common language, for executing adaptive control in different situations where there is a lack of certainty regarding the actions and outcomes, such as during planning. The behavioral paradigm that we propose in this protocol has been used to study cognitive planning and its temporal and neural characteristics. Although various mechanisms for cognitive control have been reported in other scenarios, the current protocol has allowed for the recent description of planning and its associated neural and temporal properties⁵⁴. The cognitive process of planning comprises two distinct phases: the mental planning phase, during which an internal representation of a sequence of plans is developed⁵⁵, and the planning execution phase, in which a set of motor actions are executed to achieve the previously planned goal⁵⁶. Planning is known to require the integration of various components of executive functions, including working memory, attentional control, and response inhibition, making the experimental manipulation and isolated measurement of these processes challenging^{57,58}.

Neuroimaging studies on cognitive planning have commonly used behavioral paradigms such as the Tower of

London^{59,60,61}; however, in order to control the confounding factors, the tasks used for studying cognitive planning can become limited and artificial, leading to less predictive and ecological validity^{62,63,64,65}. To overcome this problem in the neuropsychology field, real-world planning situations have been proposed as ecological tasks^{62,63}. The Zoo Map Task subtest in the Behavioral Assessment of the Dysexecutive Syndrome battery measures planning and organizational skills in a more natural and relevant manner^{64,66}. This test is a pencil-and-paper test that involves planning a route to visit 6 out of 12 locations on a zoo map. The locations are common places that can be found in a regular zoo, such as an elephant house, lion cage, rest area, coffee shop, etc. There are two conditions that evaluate different levels of planning: i) the formulation condition, where the subjects are instructed to plan a route to visit six places in the order of their choice but according to a set of rules; and ii) the execution condition, where the subjects are instructed to visit six places in a specific order and following a set of rules as well. These two conditions provide information about planning skills in ill-structured (formulation) and well-structured (execution) problems⁶⁷. The first is presented as a more demanding cognitive task in an open situation because it requires subjects to develop a logical strategy to achieve the goal. Before tracing a path, a sequence of operators must be devised; otherwise, errors are likely to occur. On the other hand, the execution condition requires a lower cognitive demand because solving a task involving following a specific imposed strategy only requires the subject to monitor the implementation of the formulated plan to achieve the goal⁶⁶. On the other hand, the Porteus Maze is a well-known task in the field of psychology, particularly in the areas of cognitive psychology and neuropsychology, and it has been widely used as a tool to assess various aspects of cognition, such as problem-solving and planning^{68,69}. The Porteus Maze task is

a pencil-and-paper task that starts with a simple visual stimuli analysis and becomes increasingly difficult. The subject must find and trace the correct path from a starting point to an exit (among several options) while following rules, such as avoiding intersecting paths and dead ends, and acting as quickly as possible⁶⁸. Each time a fork appears while drawing the path, the subjects make decisions to reach the goal and avoid breaking the given rules⁶⁹.

Considering the limitations and strengths of the commonly used and ecological tasks, we designed our behavioral paradigm mainly based on the Zoo Map Task⁶⁶ and the Porteus Maze Task⁶⁸. The behavioral paradigm consists of four distinct stages that encompass the cognitive process of planning in a daily life scenario. These stages are as follows: Stage 1, planning, where the participants are tasked with creating a route to visit various locations on a map, ensuring adherence to the established rules; Stage 2, maintenance, where the participants are required to keep the planned route in their working memory; Stage 3, execution, where the participants execute their previously planned route by drawing and closely monitoring its accuracy; and Stage 4, response, where the participants report the sequence of animals visited according to their planned route⁵⁴. Our paradigm enables the measurement of different parameters of planning ability using different stages, which reflect the various components of planning (such as working memory, executive attention, and visuospatial skills) in a more realistic manner since mapping out routes is a common occurrence in daily life. Additionally, to control for confounding factors, the paradigm includes a control task with a planning task structure and equivalent stimuli, which engages the executive cognitive components also involved in planning but excludes the planning process component. This allows for the separation

of the planning process component for the comparison of both electrophysiological markers and behavioral parameters⁵⁴.

Furthermore, eye-tracking has made significant contributions to cognitive neuroscience studies by providing a non-invasive method for measuring and analyzing eye movements, which can provide valuable insights into the cognitive processes and neural mechanisms underlying perception, attention, and cognitive functions. Measuring different types of eye movements with an eye-tracking system can provide valuable information about the cognitive processes and neural mechanisms involved in planning. For example, the following aspects can be measured: fixations, which are the periods of stable gaze during which visual information is acquired⁷⁰; saccades, which are the rapid eye movements that are used to shift the gaze from one location to another⁷¹; smooth pursuit, which is a type of eye movement that allows the eyes to follow a moving object smoothly⁷²; microsaccades, which are small, rapid eye movements that occur even during fixations⁷³; and blinks, which are a reflex action that helps to keep the eyes lubricated and protect them from foreign objects⁷⁴. These eye movements can provide insights into the cognitive processes involved in visual search, attention allocation⁷⁰, visual tracking⁷², perception⁷³, and working memory⁷⁴, which are important components for planning and cognitive control.

On the other hand, recent studies on the locus coeruleus-norepinephrine (LC-NE) system have shown its relevant role in cognitive control⁷⁵. The locus coeruleus (LC) projects to several brain regions, such as the cerebral cortex, hippocampus, thalamus, midbrain, brainstem, cerebellum, and spinal cord^{76,77,61}. Particularly dense LC-NE innervations receive PFC brain areas associated with cognitive control⁷⁵. Besides, some studies indicate that

chronic hyperactivity of the LC system may contribute to symptoms of manic-depressive disorder, such as impulsivity and sleeplessness. In contrast, a chronic decrease in LC function has been linked to reduced emotional expression, a prevalent characteristic among patients suffering from depression⁷⁸. An overactive response of the locus coeruleus to stimuli may lead to an excessive response in individuals with stress or anxiety disorders⁷⁹. Therefore, alterations in the LC-NE system may contribute to the symptoms of cognitive and/or emotional dysregulation. Non-invasive techniques can be used to examine locus coeruleus activity, one of which is pupil diameter changes, which are mostly controlled by noradrenaline released from the locus coeruleus. Noradrenaline acts on the iris dilator muscle by stimulating the alpha-adrenoceptors and on the Edinger-Westphal nucleus, which sends signals to the ciliary ganglion and controls iris dilation through the activation of postsynaptic alpha-2 adrenoceptors^{66,80,81,82}. Direct LC neuronal recordings from monkeys have confirmed the relationship between LC-NE activity, pupil diameter, and cognitive performance⁸³. Pupil dilation has been repeatedly observed in response to enhanced processing demands in several cognitive tasks^{71,84,85,86,87}.

Electrophysiological markers of cognitive control combined with eye tracking and pupillary recordings might disentangle crucial questions about how cognitive control and planning are implemented in the brain. The importance of using our protocol combining EEG and eye-tracker systems is two-fold. On the one hand, cognitive control seems to require the participation of distributed brain activity in precise temporal relationships, which constitute ideal candidates for studying brain network function. On the other hand, abnormalities in any of these capacities have a severe impact on normal behavior, as might be in the case

of a variety of cognitive and neuropsychiatric disorders, such as attention-deficit/hyperactivity disorder^{88,89}, major depressive disorder^{90,91}, bipolar disorder⁹¹, schizophrenia⁹², frontotemporal dementia⁹³, as well as disorders due to frontal lesions⁹⁴. Additionally, the current protocol allows for using pupillometry as a parameter to compare LC-NE activity and oscillations using eye-tracking and electroencephalography. This might not only provide evidence for the theoretical relationship between LC-NE, pupillometry, and neural markers in humans but could also permit the tracking of the developmental trajectory of characteristics related to the LC-NE system during cognitive planning. However, in our model, we focused on testing whether there was a specific pattern of saccades during planning that could potentially result in specific oscillation changes⁹⁵. Additionally, we used an eye-tracker system as an important part of examining the behavioral execution of a plan in the execution phase of our behavioral paradigm.

To sum up, this protocol might produce testable models of brain network dynamics that could serve as a platform for both further basic research and eventual clinical and therapeutic applications.

Protocol

All procedures in this protocol were approved by the bioethics committee of the Faculty of Medicine of Pontificia Universidad Católica de Chile, and all participants signed an informed consent form before the beginning of the study (research project number: 16-251).

1. Participant recruitment

1. Recruit right-handed healthy adults (males and females) with normal or corrected-to-normal vision, and screen them on the inclusion/exclusion criteria.

NOTE: In this study, 27 healthy individuals who were aged between 19 years old and 38 years old and were fluent speakers were recruited. The sample size can vary based on the desired level of statistical power, and the age range may vary depending on the specific research question to be addressed. In our protocol we calculated the sample size by taking into account the statistical Wilcoxon signed-rank test, an effect size of 0.7, an alpha level of 0.05, and a power of 0.95, as described in Faul et al.⁹⁶. We used the MINI-International Neuropsychiatric Interview⁹⁷, applied by a trained psychologist, to assess the participants in terms of the inclusion/exclusion criteria. Recruit only right-handed subjects to reduce variability in the EEG signal because left-handed individuals might present a different topographical distribution of EEG activity^{98, 99, 100}.

2. Stimuli preparation

1. For the planning task, create a set of stimuli using a vector graphic editor software (see **Table of Materials**). For each stimulus, design a grayscale maze that represents a zoo map. Inside the maze, make a gateway and several paths leading to the animal locations (e.g., in this study, there were four animal locations, see **Figure 1**).

NOTE: In this study, we created 36 mazes in which each stimulus consisted of a zoo map with a starting gate, four images of animals located on the maze, and several paths. The paths on the maze may or

may not lead to the animal locations. Using grayscale stimuli with reduced contrast is often preferred for pupillometry because it reduces the stimulation of the retinal cones, which are responsible for color vision. This shift in stimulus emphasis allows for a more sensitive measurement of changes in the size of the pupil, which are thought to reflect changes in the state of arousal or attention. Additionally, the use of grayscale stimuli reduces variability in the measurement due to differences in color vision between individuals¹⁰¹.

2. In order to obtain different levels of complexity in the final task, divide the stimuli based on the number of valid solutions in accordance with the established goal and rules (particularly, the goal is to plan a path to visit animal locations). The number of valid solutions refers to the number of paths possible to plan following the rules (see rules in **Figure 2** and step 5.12.1.). Classify stimuli with greater than five possible solutions as "easy" and those with five or fewer possible solutions as "difficult." Then, create an equal number of trials for each category.

NOTE: Alternatively, request the stimuli created for Domic-Siede et al.⁵⁴ from the authors, as those stimuli were created following these instructions. Consider that all the materials are available upon request, but the specifications are detailed here. In this study, we created 18 easy trials and 18 difficult trials. Evaluating the differences in difficulty levels at behavioral and electrophysiological levels is important because it will help to determine if you are measuring cognitive demand/cognitive effort/difficulty or intrinsic aspects of cognitive planning (see representative results and discussion sections).

3. For the control task, use the same structure as the planning task (evaluation period, maintenance,

execution, response, see **Figure 2**), and use the same stimuli created for the planning task, but add a drawn line representing a marked path for visiting the sequence of animal locations starting from the gate until the last location (see **Figure 1B**). Make the marked path a slightly darker color than the main paths of the maze, with low contrast evaluated using a lux-meter (see step 2.4).

NOTE: The idea behind this is to keep the psychophysical features of both conditions (planning and control tasks) as similar as possible. The traced paths of the mazes could either follow the rules or not (see section 5 of the protocol for more detail regarding the instructions given to the participants). In this study, half of the stimuli had a correct visiting sequence following the rules, whereas the other half presented errors (such

as using the same path twice or crossing dead ends, see step 5.12.1 and step 5.12.3 and **Figure 2**).

4. Assess the illuminance of the stimuli using a lux-meter positioned in the chinrest that the subjects will use (see step 4.5 and step 4.6) and at the same distance from the screen. Each stimulus of each condition produces a lux value. Record each value manually for further analyses. **NOTE:** No differences in illuminance are expected between conditions (see step 4.6). Otherwise, check the contrast of the stimuli. This is relevant if pupil diameter will be measured¹⁰².
5. Create one stimulus representing correct feedback (thumbs-up when correct) and another stimulus representing incorrect feedback (thumbs-down when incorrect) using a vector graphic editor (see **Table of Materials**) as well (**Figure 2**).

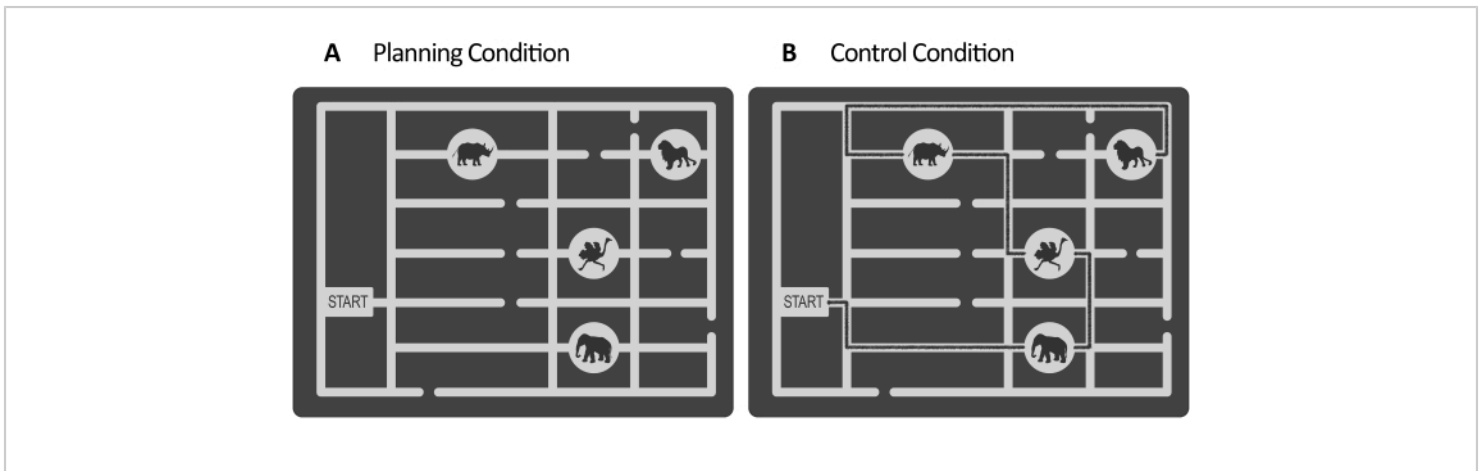


Figure 1: Stimuli of the experimental and control task. Illustrative examples of the (A) planning and the (B) control task stimuli are shown. The stimuli represent a zoo map consisting of a gate, four animal locations in different places, and several paths. The stimuli for both conditions were similar; the only difference was that for the control task, (B) the stimuli had a marked line indicating an already existing path (black line here for illustrative purposes). This line in the real control stimuli was slightly darker, with low contrast controlled by illuminance (see step 2.4). This figure has been modified from Domic-Siede et al.⁵⁴. [Please click here to view a larger version of this figure.](#)

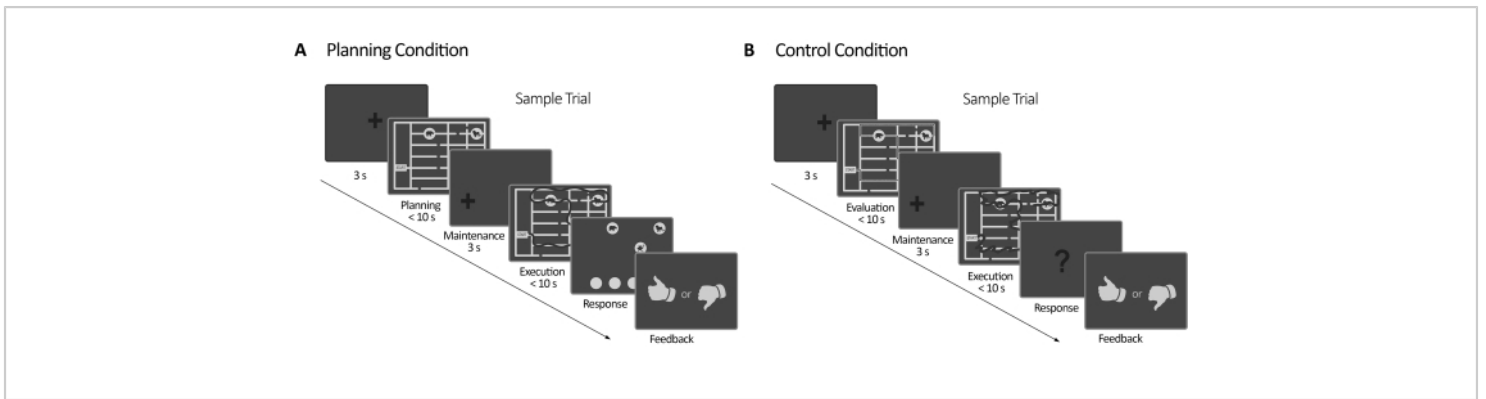


Figure 2: Experimental design. (A) Planning task trial. Trials in this condition started with a 3 s fixation cross. Then, the participants were instructed to plan a path to visit all the four animal locations following a set of rules (10 s maximum). Next, a shifted fixation cross appeared (3 s), followed by the appearance of the maze again. In this period (execution), the subjects had to execute the trace planned in the previous planning period using their gaze with online visual feedback (given by the eye-tracker system), which delineated their gaze movement in real-time (dark line) (10 s maximum). Afterward, in the response period, the subjects had to report the sequence made during the execution by ordering the animals visited. According to their responses, feedback was delivered. (B) Control task trial. Trials in this condition started with a 3 s fixation cross. Then, the participants were instructed to evaluate whether a traced path (dark line) followed the rules or not. Next, a shifted fixation cross appeared (3 s), followed by the appearance of the maze again. In this period, the subjects had to redraw the already traced path with online visual feedback, like in the planning execution period (10 s maximum). Afterward, in the response period, the subjects had to answer (yes or no) whether the traced sequence followed the previously stated rules. According to their responses, feedback was delivered. This figure has been modified from Domic-Siede et al.⁵⁴. [Please click here to view a larger version of this figure.](#)

3. Planning and control task programming

1. Write a script coding a planning task paradigm based on the Zoo Map Task⁶⁶ and Porteus Maze⁶⁸ using a stimuli presentation/behavioral experiments software (see **Table of Materials** and the **Supplementary File**).
 1. Code the task considering two conditions (a planning condition and a control condition) with a similar structure to that explained in section 2 and section 4 (see **Figure 2** and the **Supplementary File**).

NOTE: It is important to use the same structure in both conditions in order to control the confounding factors and perceptive components involved in the process of solving the task demands (**Figure 2**). Using the same structure improves the assessment of the specific cognitive process involved in cognitive planning.

2. Synchronize the communication between the display computer, the EEG computer, and the host computer (eye-tracker computer) *via* ethernet and parallel port communication sending transistor-

transistor logic (TTL) pulses from the display computer (see **Figure 3**).

3. Write a code to calibrate the eye movements with the eye-tracker system at the beginning of the planning and the control tasks and after every five trials completed because gaze position on the screen is crucial for the execution period (see step 3.2.3 and step 3.3.3 of the protocol, the discussion section, and the code in the **Supplementary File**).

NOTE: There might be delays in the computer communication. There are several methods to measure the delay between TTL pulses on two different computers, but one common approach is to use a hardware device such as a digital oscilloscope or a logic analyzer. Another approach is to use software-based methods, such as sending the TTL pulses over a network connection and using network analysis tools to measure the delay. Another approach is to synchronize the clocks of the two computers, either using a global positioning system (GPS) or network time protocol (NTP) server or using a hardware-based synchronization solution, calculate the delay between the timestamp and the time of arrival for each pulse, and average the results to obtain the overall delay between the two computers.

2. Write a code for the planning task with the following structure: the planning period, the maintenance period, the planning execution period, the response period, and feedback (**Figure 2, Supplementary File**).
 1. **The planning period:** Initiate the planning condition by setting a fixation cross presented for 3 s as a baseline.

2. Randomly present the set of mazes one by one (36 in this study).

NOTE: In this planning period, participants are asked to plan a path to visit the four animal locations, with a maximum time of 10 s, following a set of rules (the rules are previously explained to them; see section 5 of the protocol to see the rules given, as well as **Figure 2**).

3. Include a TTL trigger in the code signaling the onset of the stimulus presentation using a tag code, and send this trigger to the EEG computer and the eye-tracker host computer for further narrower and windowed analyses.

4. Write in the code that the planning period culminates once a button from a joystick/keyboard is pressed whenever the subject finishes planning or if the maximum time is exceeded. The reaction time (RT) must be recorded in the logfile for further analyses.

NOTE: For this period, we used a trigger code using the number 1, but the use of hierarchical event descriptors (HED) tags over numerical codes is recommended, because HED tags provide meaning and structure to the content, thus making it easier for other researchers or collaborators to understand the content of the data.

5. **The maintenance period:** Initiate this period using a shifted fixation cross presented for 3 s. Locate the shifted fixation cross in the spatial position where the gate of the maze is located in order to anticipate the start position (gate) of the zoo map (see **Figure 2**).

NOTE: The purpose of this period is three-fold. First, the shifted fixation cross facilitates the execution of the trace representing the planned path for the next

- period (see step 3.2.8). Second, during this period, the participants hold the plan elaborated during the planning period in their working memory. Finally, this period serves as an inter-trial interval to delimitate the end of the planning period and the beginning of the next period-the planning execution period.
- The planning execution period:** After shifted fixation cross is shown for 3 s during the maintenance period, present the maze again.
 - Send a TTL trigger to the EEG and the host eye-tracker computer to indicate the beginning of this period using a specific tag code.
 - Write a code to give real-time visual feedback (a dark line, see the execution period in **Figure 2**) of the subject's gaze position approximately 992 ms after the onset of this period.
NOTE: Starting to delineate with a delay (1,000 ms approximately) gives the subjects time to become oriented in the maze, allowing them to delineate their previous planned path (during the planning period) with a dark line.
 - Record the coordinates of the paths for further reconstruction of the paths made by the subjects, and score the performance offline (see step 6.1.1, **Figure 4**).
 - Ensure a maximum time of 10 s to trace the planned path, and allow the subjects to finalize this period by pressing a button. In this way, the subjects can control when they have finished their drawn path.
 - Save the RT in the logfile for further analyses.
 - The response period:** Write a code for the response period, which starts after 10 s of planning execution or upon a button press at the end

of the planning execution period, in which the maze disappears but the animals and their spatial positions remain on the screen.

- Place four empty circles horizontally at the bottom of the screen in the response period.
NOTE: The purpose of this period is to allow the subjects to indicate the sequence of animals visited during the planning execution period by putting the animals into the circles in the same order in which they visited them using a joystick or keyboard.
- Configure the program/code to allow the subjects to use the joystick or keyboard to select each of the animals (four animals in this study) presented before and insert them into each of the four circles (see **Supplementary File** and **Figure 2**).
- Feedback:** Write a code to deliver 3 s of feedback to the participants. A thumbs-up image should be displayed in response to valid combinations of animals visited if the rules are followed, while a thumbs-down image should be displayed if the combination reported is invalid.
- Send a TTL trigger, using a specific tag code for correct feedback and another tag code for incorrect, to the EEG and eye-tracker computers.
NOTE: The reason for giving feedback is to facilitate the monitoring of performance and maintain motivation during the task. This provision of real-time feedback enhances the reward effect and encourages proper task performance¹⁰³.
- Write a code for the control task with the same structure as the planning condition: a control period, a maintenance period, a control execution period, a

response period, and feedback (see **Supplementary File, Figure 2**).

1. **The control period:** Write a code for the control condition period to mitigate confounding factors. The code for this period must start with a fixation cross presented for 3 s as a baseline.

NOTE: Since the planning task predominantly demands the implementation of planning but also recruits other cognitive domains as part of executive function, such as visuospatial function, working memory, attentional control, inhibitory control, etc.^{66,88,104,105}, a control task is crucial to mitigate confounding factors. Thus, the main goal of this task is to demand all the cognitive and perceptual functions needed to solve the planning task while removing the implementation of cognitive planning⁵⁴.

2. Randomly present the mazes of the control condition one by one (mazes with a marked path already traced). Code a maximum time of 10 s.
3. Include a TTL trigger in the code signaling the onset of the stimulus presentation using a tag, and send this trigger to the EEG computer and the eye-tracker host computer.
4. Write in the code that this control period culminates once a button from a joystick/keyboard is pressed whenever the subject finishes or if the maximum time is exceeded.

NOTE: Subjects are instructed to evaluate the marked paths (whether they are following the rules or not, see step 5.12 for details on the instructions given to the participants).

5. Save the reaction time (RT) in the logfile for further analyses.
6. **The maintenance period:** Once the control period has ended, present a shifted fixation cross for 3 s.
7. As the planning execution period, place the fixation cross where the gate entrance is located to facilitate gaze drawing for the next period.
8. **The control execution period:** Present the maze again, and simultaneously send a TTL trigger to the EEG and host eye-tracker computers with a tag signaling the onset of the execution period.
9. Repeat the same code as for the planning execution period to give online feedback of the gaze position and to delineate and overlap their gaze with the traced path.
10. Ensure a maximum time of 10 s to trace the path, and allow the subjects to finalize this period by pressing a button.
11. Save the RT in the logfile for further analyses.
12. **The control response period:** Once the control execution period has ended, present a question mark indicating the response period.
13. Program two buttons, respectively, for the subjects to give a response using a joystick or a keyboard.
NOTE: Here, the subjects are asked to answer whether the sequence marked by the trace was correct or not by selecting one button for correct/YES and another for incorrect/NO.
14. Save the accuracy in the logfile.
15. **Feedback:** Write a code to deliver 3 s of correct feedback whenever the subjects respond correctly (a thumb-up image) and deliver 3 s of incorrect

feedback when the subjects respond incorrectly (a thumbs-down image).

16. As in the planning condition, send a TTL trigger to the EEG and host eye-tracker computers with a tag for correct feedback and another tag for incorrect feedback.

4. **Training tasks:** Create stimuli, write a code, and present before the aforementioned planning and control tasks a

brief training session of approximately six trials/mazes for each condition (planning and control)

NOTE: The idea is to ensure familiarization with the task setting. It is recommended to set criteria for proceeding. In this study, if the last three trials were correct, and the participants reported understanding the goal and the procedure at the end of the training session, the participants then proceeded to the experimental session.

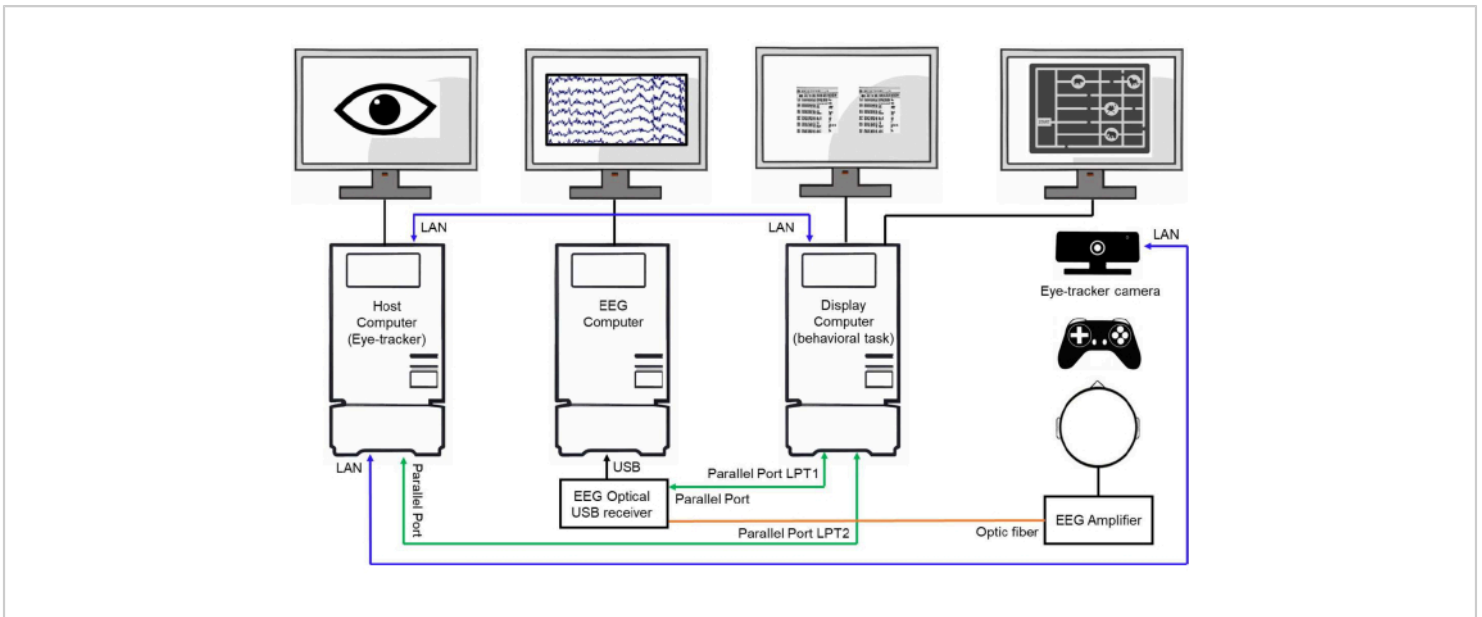


Figure 3: Example of a laboratory setup. Schematic representation of a laboratory setup showing three interconnected computers. The host computer (eye-tracker computer) is responsible for tracking and storing the eye movement data. The EEG computer acquires and stores the EEG signals. The display computer controls the behavioral experiment, presents the stimuli to the subjects, and sends event triggers to the host and EEG computers through parallel ports and LAN connections to synchronize the data collection. [Please click here to view a larger version of this figure.](#)

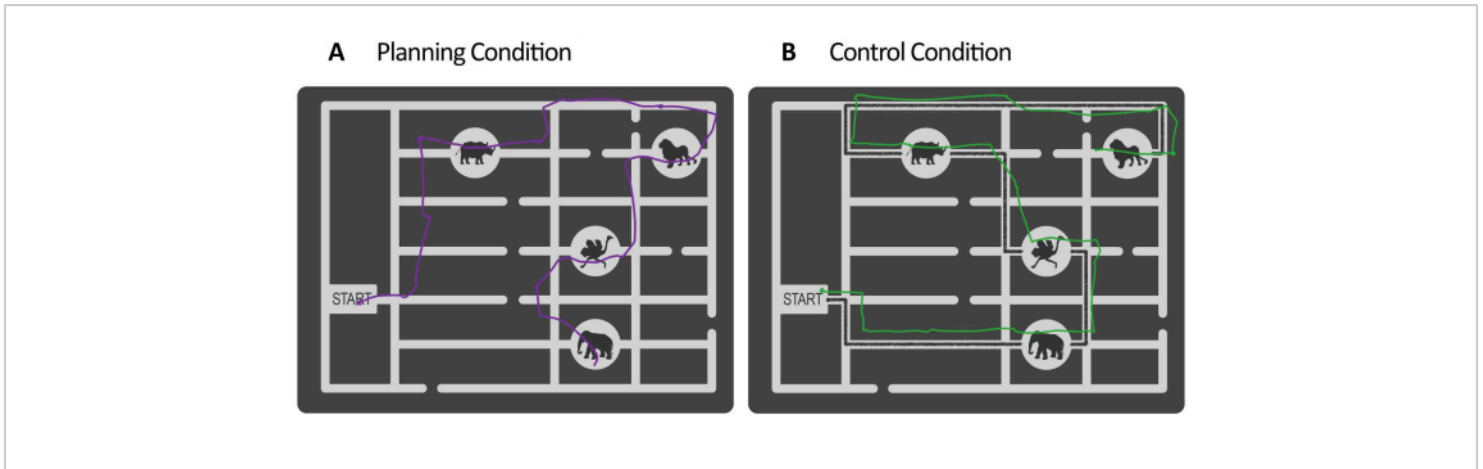


Figure 4: Path reconstruction from visual online feedback given by the eye-tracker system. Illustrative examples of a path reconstruction from the motor execution of a plan (**A**, in purple, planning execution period) and a control execution period (**B**, line in green) and with eye-tracker data. The path reconstructed in the planning execution period is used to evaluate the accuracy of each planning task trial. [Please click here to view a larger version of this figure.](#)

4. Laboratory setting and equipment

1. Use an EEG acquisition system to record EEG activity from the participant's scalp, with the EEG electrodes placed according to the international 10-20 system¹⁰⁶. Position two electrodes on the participant's mastoids for offline re-referencing. Use electrooculogram electrodes to identify vertical, horizontal, and blink eye movement signals during visual inspection.
2. Use EEG acquisition software for the EEG data acquisition with a sampling rate of 2,048 Hz or 1,024 Hz and a band-pass filter between 0.1-100 Hz in the EEG computer.
NOTE: Sampling rates of 1,024 Hz and 2,048 Hz provide enough resolution to analyze low-frequency oscillations. It is important to acquire EEG signals with a high sampling rate, such as over 1,000 Hz, when analyzing low-frequency oscillations in order to ensure that the low-frequency signals are not aliased.
3. Use a display computer, which is connected with the EEG computer and the host eye-tracker computer *via* parallel ports and ethernet and has a platform to run behavioral experiments installed on it, to project the stimuli onto an extended monitor with a minimum resolution of 1,920 pixels x 1,080 pixels and a refresh rate of 60 Hz. Place this monitor approximately 82 cm away from the subject.
NOTE: We used a 24 in monitor with a refresh rate set at 144 Hz located 82 cm away from the participant. It is recommended to use a monitor with a screen size of at least 19 in for cognitive experiments involving recording EEG and eye movements. Additionally, a general recommendation is to place the monitor at a distance that allows the participant to comfortably perform the task and maintain a stable gaze on the screen while still allowing for accurate recordings of EEG

and eye movements. It is advisable to test and adjust the setup as necessary to ensure the best results.

4. Use an eye-tracking system to give the participants real-time feedback on their eye movements during the execution periods, and record the pupil size. Set the sampling rate at 1,000 Hz for an adequate temporal resolution.
5. Avoid head movements. Left and right and up and down head movement restrictions are needed to keep the eye within the video camera's field of view. Forward and backward movement restriction is needed to keep the eye in the video camera's focal range. Use a combination of forehead/chin rests to keep movements within this range.
6. Evaluate the luminance of the stimuli using a digital lux-meter or similar to compare differences between the planning stimuli and control stimuli.
NOTE: A statistical test such as a t-test or Wilcoxon can be used to evaluate differences between the stimuli of the two conditions.
7. Use a control joystick or keyboard with at least four buttons: two buttons for Yes/No questions from the control condition; one of these two buttons to finish trials; and another two buttons for the response period of the planning condition to move forward or backward to insert the animals into each of the four circles at the bottom of the screen.

5. Electroencephalography and eye-tracking recording sessions

1. Before starting the study, have the participants complete written and signed informed consent.

2. Prior to the recording session, ask the participants not to attend wearing makeup (mascara and eyeliner can be detected as a pupil by the eye-tracker system), having taken drugs or caffeine^{107,108}, or if they feel severe fatigue¹⁰⁹ (stress, sleep deprivation, etc.).
3. Have participants complete a demographic survey to provide information on their sex, age, handedness, native language, and neuropsychiatric history *via* the MINI-International neuropsychiatric interview⁹⁷ applied by a trained psychologist.
4. Clean the subject's forehead, scalp, mastoids, and electrooculogram (EOG) skin position with an alcohol wipe.
5. Place all the external electrodes on the participant. Put the horizontal EOG bipolarly on the outer canthi of both eyes and the vertical EOG above and below the participant's right eye. Put two external electrodes on the right and left mastoid for later re-referencing.
6. Measure the subject's head, and place the correct-size EEG cap according to the extended international 10-20 system. In order to do this, find and place the Cz electrode following these steps:
 1. Identify the midline of the scalp by visually inspecting the hairline and the top of the nose. Identify a line connecting these two points to define the midline.
 2. Locate the Cz. The Cz is typically defined as the midpoint between the two preauricular points (i.e., the points located just in front of each ear). Locate these points, and then identify a line connecting them to identify the approximate location of the Cz.
 3. Measure and mark the Cz. Measure the distance from the nasion (i.e., the bony protuberance at the

top of the nose) to the Cz. The distance from the nasion to the Cz is typically around 53% of the total head circumference in the 10-20 system. Mark the location of the Cz using a pen or another marking tool.

NOTE: It is important to follow a consistent and standardized procedure for electrode placement in order to minimize errors and ensure the validity of the EEG data. It is recommended to develop a standard placement procedure. Create a standard procedure for placing the electrodes on each subject's scalp, and ensure that the same procedure is used for every subject. In case there is a team or staff performing the recordings, train the technicians or research assistants on the proper placement procedure to ensure that they consistently and accurately place the electrodes. Furthermore, digitizing the electrode positions for each subject would be a desirable approach in order to perform source analysis later. In EEG studies, the precise three-dimensional (3D) location of each electrode on the subject's head is frequently a requirement for establishing a correlation between the EEG data and the corresponding brain activity¹¹⁰. This information is also critical for the proper alignment of the EEG data with anatomical images derived from MRI or CT imaging techniques^{111, 112}.

7. Insert conductive gel into each hole of the cap using a syringe with a blunted needle, moving away the participant's hair with the tip. Afterward, put all the scalp electrodes on the EEG cap.
8. Check the impedances using the EEG recording software, and make sure they are under the resistance level recommended by the EEG system.

9. Ask the participant to stay as still as possible during the experiment. Inspect the EEG signal, and test it by asking the participant to blink, make a jaw, and remain a few seconds with the eyes closed.
10. Seat the participant in a dark and sound-attenuated room. Use a chin rest to stabilize their head and minimize movement, and check that there is a distance of approximately 82 cm between the chin rest and the center of the stimulus-presentation screen.
11. Place a joystick or keyboard in front of the participant for the responses.
12. **Instructions:** Give oral instructions using visual aids before starting each condition (planning and control). In the instructions, include visual examples of the stimuli, and explain how to solve the mazes in the planning and the control conditions, respectively.
 1. For the planning task, instruct the subjects to find a path to complete a sequence of visits to certain animal locations (four locations in this study) in different places of the maze in any order and following a set of rules: "(1) Plan the path as fast as possible within a maximum of 10 s; (2) Start from the gateway, and conclude the path at the fourth animal visited; (3) Do not pass through the same path or corner twice; (4) Do not cross a dead end; (5) Do not cross a path perpendicularly"⁵⁴.

NOTE: For rule 2 to rule 5, we recommend showing visual examples to the participant.

2. Afterward, start the planning task training session of six trials.

NOTE: Instruct the participants to report before each eye-tracker calibration period if there was any problem performing the task, especially during

delineating the path in the execution period. Take a note of whether there was a trial to check offline/post-processing (see step 6.1.1).

3. For the control condition, instruct the subjects to evaluate whether the already marked path on the maze has been made correctly or incorrectly considering the rules previously learned.

NOTE: Give examples with visual support of how to evaluate the mazes without using planning strategies, such as not trying to plan a new path when errors are detected (such as drawings using the same path twice, crossing a dead end, etc.). When an error is found, the focus should be solely on reporting the detection of the error rather than correcting the path. After each trial, ask the participants about the strategies they implemented. Then, provide oral feedback about their performance to make sure that they evaluated the paths drawn and avoided planning new paths. Afterward, start the control task training session of six trials.

13. Check the EEG signal to make sure that all the channels are correctly being acquired. Start the EEG recording.

14. Calibrate the eye tracker.

NOTE: Verify the capability of the eye tracker to determine the gaze position when the participant directs their gaze to various regions of the screen.

1. Inform the participant that the eye tracker will be calibrated and that they are going to see a white circle (with a small gray dot) moving randomly to the four corners of the screen (five-point calibration procedure). Instruct them to fixate their gaze in the circle, and inform them that, when it moves to another location, they should follow the circle's

position and fixate their gaze again in that new position.

2. Run the experiment, start saving the eye movements by clicking on **Output/Record**, and ask the participant to follow the instructions previously given, informing them the experiment will now begin.
3. Keep the laboratory room in a dark environment. The largest changes in pupil dilation occur in response to changes in luminance¹¹³. Maintain a consistent light level in the experimental environment.

6. Data analyses

1. Behavioral analyses

1. Analyze the behavioral data using statistical software (see **Table of Materials**). Measure the accuracy (percentage rate of accurate responses) as a quantitative behavioral parameter in both the planning and control conditions. For the planning condition, use eye-tracker data (x and y coordinates of gaze position) to recreate the paths taken during the execution period offline, and determine the accuracy of the planned paths compared to the actual traced paths (**Figure 4**). To do this, manually check the congruency between the combinations correctly/incorrectly made in the response period and the trace made.
2. Calculate the RT, which is the mean time spent solving the mazes for the planning period and the mean time spent evaluating the marked paths for the control period.
3. Calculate the mean RT of the execution periods for the planning and control conditions. Specifically, use the RT corresponding to only the correct trials.

NOTE: Complementarily, it is possible to use the linear integrated speed-accuracy score (LISAS)^{114,115} described in Domic-Siede et al.⁵⁴, which provides a combined measure that considers reaction time and accuracy. As the reaction time during the planning execution period and the accuracy of planning are interrelated, the LISAS can be utilized to compute an index that accounts for the reaction time corrected for the number of errors made. Additionally, the LISAS index can be used to assess the correlation between electrophysiological signals and behavioral performance as well. It is calculated as a linear combination of reaction time (RT) and error proportion (PE).

4. Evaluate the homoscedasticity using a statistical test such as the Levene Test^{116,117}, and test the normality using the D'Agostino and Pearson omnibus normality distribution test¹¹⁸ or Shapiro Wilk test¹¹⁹ to choose the proper statistical test for comparisons (parametric or non-parametric).
5. Evaluate whether the planning component in the planning condition is more cognitively demanding than the control condition using either the Wilcoxon signed-rank test¹²⁰ or the matched-pair t-test¹²¹ to compare the behavioral parameters between the conditions.

NOTE: In this way, validate that the behavioral paradigm is optimal to evaluate cognitive planning.

6. Separate the trials in the planning condition into "easy" and "difficult" categories (refer to step 2.2), and then use a matched-pair t-test to compare the accuracy and reaction times in the planning and

execution periods between the "easy" and "difficult" trials.

2. EEG and eye movement pre-processing

1. Perform the EEG data pre-processing pipeline explained in the following points using self-made scripts and/or established toolboxes, such as those described in Delorme and Makeig¹²², in Dimigen et al.¹²³, and in Mognon et al.¹²⁴, in a programming language software (see **Table of Materials**).
2. Synchronize the eye movement activity with the EEG recordings to import the fixations, saccades, and blink events for better visual inspection or further analyses (see step 3.1.2 and the **Supplementary File**).

NOTE: In this study, we used the timestamps on the eye-tracking data and the time stamps on the EEG data as described in Domic-Siede et al.⁵⁴ and in Dimigen et al.¹²³ to import the eye movement events to the EEG data in a programming language software.

3. Down-sample the data to 1,024 Hz in case they were recorded at 2,028 Hz to reduce the computational demands.

NOTE: A sampling rate of 1,024 Hz is sufficient according to the frequency range of interest of 4-8 Hz, the expected frequency resolution, and the computational requirements of the analysis.

4. Re-reference the EEG signal to the average of the electrodes on the mastoids.

NOTE: Other references are possible. The choice of reference can impact the results of the EEG analysis and the interpretation of the data, so it is important to carefully consider the pros and cons of different

referencing options. The average mastoid reference is a popular choice for EEG studies because it provides a stable reference that is easy to calculate, and it has been shown to be effective for analyzing many different EEG signals. Referencing the EEG data to the average of the mastoids (known as the average mastoid reference) is a common approach for analyzing frontal theta activity in scalp EEG data. The mastoid electrodes are located near the ear and provide a reference for the EEG signals. Referencing to the average of the mastoids can help to reduce the influence of noise and artifacts that are not of interest while avoiding canceling the signal of interest, which helps the user to obtain a clearer representation of the EEG signals.

5. Apply a zero-phase finite impulse response (FIR) with a high-pass cut-off frequency of 1 Hz and a low-pass cut-off frequency of 40 Hz over the extended signal (without epoching) using a programming language software.

NOTE: In this study, we used the toolbox described in Delorme and Makeig¹²².

6. For each condition, considering the number of trials, divide the data into epochs centered around the start of the planning and control periods, respectively. Use the 1 s prior to the start of the maze presentation as the baseline and 4 s after the planning or control period as the segments of interest. Use a programming language software.

NOTE: In this study, we used the toolbox described in Delorme and Makeig¹²² and 36 epochs/trials.

7. Create a second segmentation centered around the end of the planning and control periods using 4 s

before the end and 1 s after as the maintenance period.

NOTE: The reason for selecting the first and last 4 s of the planning and control periods (step 6.2.6 and step 6.2.7) is that the duration of each period in both conditions can vary, and analyzing the first and last seconds of planning can provide a more comprehensive view of the planning process. Thus, these window lengths are adequate and sufficient to analyze the oscillatory dynamics underlying planning.

8. Over the segmented signal, run the Logistic Infomax independent components analysis (ICA) algorithm¹²⁵ to identify and remove artifactual components.
9. Use the saccade-to-fixation variance ratio criterion recommended in Plöchl et al.¹²⁶ to automatically detect potential noisy components, and use the automatic EEG artifact detector based on the joint use of spatial and temporal features recommended in Mognon et al.¹²⁴.

NOTE: We recommend the use of the independent component classifier proposed in Pion-Tonachini et al.¹²⁷, which estimates independent component classifications as compositional vectors across seven categories, helping to identify artifacts.

10. Inspect other potential artifactual components such as EMG, electrode movement, or non-brain-related components. Validate the rejection of these components by visually inspecting the topographies, spectra, and activations over time.

11. Interpolate (spherical interpolation) noisy channels by automatic channel rejection using the kurtosis criterion (with a z-score of 5 as the threshold).
3. Time-frequency analyses
 1. Perform a short-time fast Fourier transform (FFT) (1 Hz to 40 Hz) using a window length of 250 ms and a time step of 5 ms. Use a Hanning window. Use the z-score to normalize the time-frequency charts to the baseline (−1 s to −0.1 s).

NOTE: The visualization of the spectrum is subject to a trade-off between the window size and the temporal resolution. To achieve a comprehensive view of the entire spectrum including the theta range of 4 Hz to 8 Hz, we recommend using the lower limit of the window size, which is 250 ms, to ensure a higher temporal resolution during each trial and task. Additionally, we recommend using a Hanning window, as this is widely regarded as a conventional choice for these cases. For better resolution in time and frequency, see the further steps.
 2. Select a time-frequency chart from a frontocentral electrode, such as the Fz, or an averaged group of frontal electrodes.

NOTE: Consider the broad evidence regarding the association between cognitive control and frontal midline theta^{12, 128, 129}.
 3. Select non-frontal control time-frequency charts from electrodes such as the Pz and Oz electrodes to further the comparisons.
 4. For the frontal and control electrodes, perform a non-parametric cluster-based permutation test for paired samples, with a *p*-value < 0.05 for the group-level comparisons of the time-frequency charts from both conditions. Use the Monte Carlo method with 1,000 random draws. Use the maximum statistic value of the cluster to perform the permutation test¹³⁰.
 5. Average the theta frequency band (4-8 Hz) from the first 4 s of planning and control, respectively, and the last 4 s segment as well.
 6. Compare the averaged theta activity between the conditions using a matched-pair t-test or Wilcoxon signed-rank test.
 7. Analyze the time profile of the theta activity. To do this, average the frequency range of 4-8 Hz across the trials by subject.
 8. Compare the theta activity dynamics between the conditions using a Wilcoxon signed-rank test matched and corrected with the false discovery rate (FDR).

NOTE: We used 88 ms steps of non-overlapping windows in the Wilcoxon test.
4. Source reconstruction
 1. Use a toolbox for source analysis reconstruction, such as the open access toolbox described in Tadel et al.¹³¹ or another similar one.
 2. Calculate the sources of the pre-processed EEG signal from the first 4 s of planning using an algorithm such as standardized low-resolution brain electromagnetic tomography (sLORETA)¹³² and the minimum-norm imaging method, as well as the symmetric boundary element method (symmetric BEM), with the help of a toolbox such as that described in Gramfort et al.¹³³ to solve the inverse problem.

3. Use the source algorithm (sLORETA algorithm in this study) on an anatomical MNI template (we used the MNI template in Brainstorm "Colin27") with the default electrode locations for each participant in case there is no 3D digitization of the electrodes (see step 5.6).

NOTE: It should be noted that using the default electrode locations is not the most efficient method for determining the sources of brain activity. However, it can still provide a general understanding of the origin of the activity. It is important to keep in mind that the localization sources obtained through these methods are rough approximations and should be interpreted with caution during the analysis of the results.

4. Apply a 4-8 Hz bandpass filter over the pre-processed signal.
5. Apply a z-score normalization using the period -1,000 ms to -10 ms before the trial onset as the baseline.
6. Average the theta activity using a time window of interest between 1 s and 4 s after the trial onset.
7. Compare the average space sources between the conditions using a non-parametric permutation sign test with Monte Carlo sampling (1,000 randomizations)¹³¹.
8. In order to determine the regions of interest (ROIs), label the cortex using a brain atlas.

NOTE: We used the Destrieux Atlas¹³⁴ implemented in the toolbox described in Tadel et al.¹³¹.

9. Select the brain regions of interest (ROIs).

NOTE: We considered the evidence reporting that the prefrontal cortex regions, such as the bilateral superior frontal gyri (SF), bilateral transverse frontopolar gyri and sulci (FP), bilateral ACC, bilateral MCC, and bilateral dorsolateral prefrontal cortex^{137,138}, are involved in cognitive control functions^{135,136}.

10. Perform principal component analysis (PCA) over the previous pre-processed EEG signal (1-40 Hz range) for each ROI, and take the first mode of the PCA decomposition for each ROI.
11. Perform a spectral analysis using a short-time fast Fourier transform, and compare the results between the left and right regions of interest using a non-parametric, cluster-based permutation test¹³⁰.
12. Extract and represent the left and right ROIs showing no differences as one bilateral time series: SF, ACC, and MCC. Then, plot time-frequency charts, and compare between the conditions.
13. Compare the time-frequency charts according to the complexity level of the planning task (easy versus difficult trials) for each ROI.
14. Mirror the edge of the signal for each of the 512 samples, and perform a bandpass filter between 4 Hz and 8 Hz for the selected ROIs.
15. Apply a Hilbert transform to obtain the instantaneous amplitude¹³⁹ using a signal processing toolbox from a programming language software (see **Table of Materials**).
16. Correct the signal using z-score normalization (-1,000 to -10 ms as baseline), and average across the trials by subject.

17. Compare each ROI theta band time profile between the conditions using the Wilcoxon signed-rank test (matched pairs, 1 s of non-overlapping windows), and correct with the FDR.
5. Correlations between EEG activity and behavioral performance
 1. Normalize the source time series of the ROIs to the baseline using the z-score. Select a window from 1 s to 4 s after the planning or control onset (where prominent theta activity in the time-frequency charts is observed).
 2. To determine the increase in theta activity in the planning condition compared to the control condition, first transform the signal into the frequency domain (1-40 Hz) using the multitaper method through a toolbox such as the Chronux toolbox¹⁴⁰ for each condition and source in the regions of interest.
 3. Compute the average frequency of the theta band (4-8 Hz), and calculate two measures of theta power: i) the difference between the theta power during the planning period ($\theta_{planning}$) and the control period ($\theta_{control}$), denoted as $\Delta \theta$, and ii) the relative increase in theta activity, expressed as the ratio of $\Delta \theta$ and the theta activity during the control period ($\theta_{control}$), as in Domic-Siede et al.⁵⁴:

$$\Delta \theta = \theta_{planning} - \theta_{control} \quad (1)$$

$$\text{Relative Increase in Theta} = \frac{\Delta \theta}{\theta_{control}} \quad (2)$$
 4. Calculate two behavioral parameters: iii) Δ LISAS planning, by subtracting LISAS control from LISAS planning, and iv) Δ LISAS planning execution, by

subtracting LISAS control execution from LISAS planning execution, as in Domic-Siede et al.⁵⁴:

$$\Delta LISAS_{planning} = LISAS_{planning} - LISAS_{control} \quad (3)$$

$$\Delta LISAS_{planning\ execution} = LISAS_{planning\ execution} - LISAS_{control\ execution} \quad (4)$$

5. Perform Spearman's rho correlations using the electrophysiological and behavioral parameters calculated, and then correct by the FDR.
6. **Eye movement analysis:** To control the potential differences in eye movements for each condition that might result in different oscillatory dynamics, perform the following analysis:
 1. Determine the saccade amplitude and the saccade peak velocity from the entire trial and from 0 s to 3.75 s during the planning and control conditions.
 2. Compare the results using either the Wilcoxon signed-rank test or the matched-pair t-test, whichever is appropriate.

NOTE: A toolbox such as that described in Dimigen et al.¹²³ can be helpful.
 3. Calculate and evaluate the coherence between the Fourier EEG power at one frontal electrode (for instance, the Fz or an averaged frontal ROI electrode) and the saccade rate as described in Sato and Yamaguchi¹⁴¹.
 4. Use the Wilcoxon signed-rank test to compare the coherence power-saccade rate values of the first 4 s of each trial between the two conditions.

Representative Results

In the present protocol, the RT of the planning period was compared to the RTs of the control period and the planning

execution period. The planning RT was greater than the control and the planning execution period RTs. Additionally, compared to the control condition, participants made more

mistakes and had lower accuracy during the planning period (Figure 5).

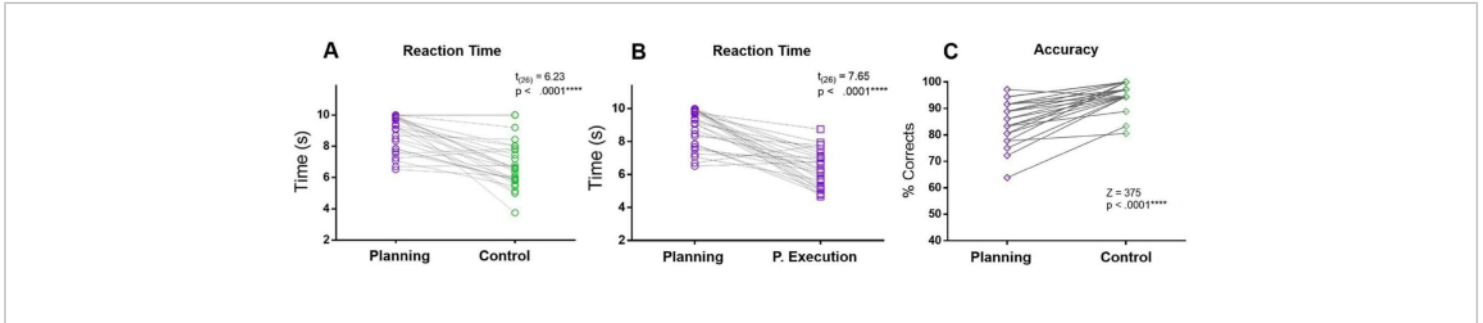


Figure 5: Reaction time and accuracy for the planning task. Comparison between the (A) reaction times in the planning period (purple circles) and the control period (green circles) using a matched-paired t-test. (B) Comparison between the reaction times in the planning period (purple circles) and the planning execution period (purple squares) using a matched-paired t-test. (C) Comparison of the accuracy rate in the planning condition (purple diamonds) and the control condition (green diamonds) using a Wilcoxon signed-rank test. This figure has been modified from Domic-Siede et al.⁵⁴. [Please click here to view a larger version of this figure.](#)

Moreover, the analysis of planning complexity levels showed significant differences in accuracy and reaction times (RTs) between the "difficult" and "easy" levels during planning and execution (Figure 6). The "difficult" level had longer RTs and

lower accuracy. These findings suggest that dividing the trials based on the number of valid solutions can distinguish "easy" from "difficult" trials.

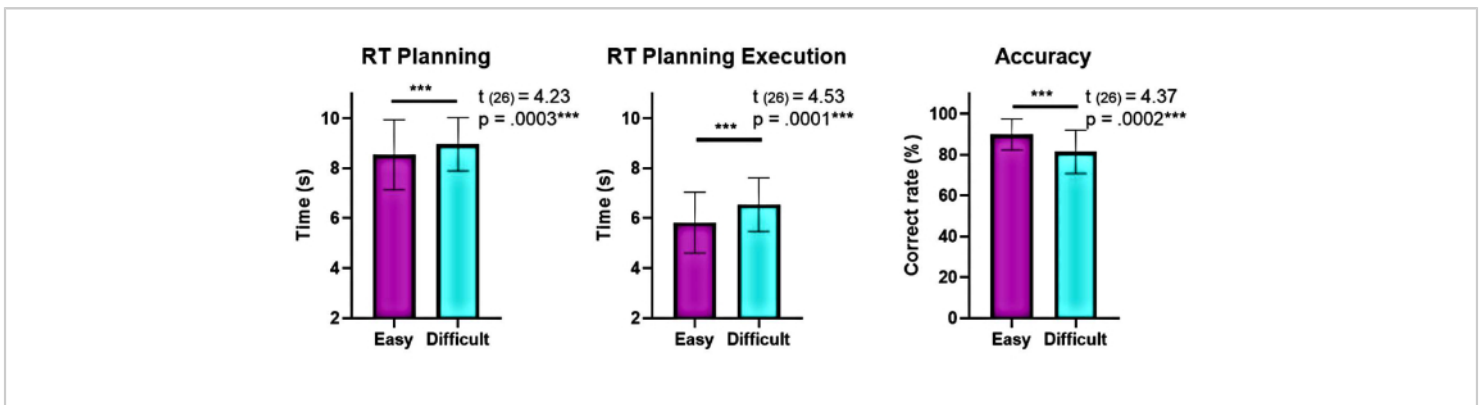


Figure 6: Comparison of behavioral performance at the different complexity levels. Significant differences in behavioral performance at the "easy" and "difficult" levels of complexity were identified using a matched-pair t-test. Lower reaction times (RTs) were seen during planning and execution for the "easy" level compared to the "difficult," and the accuracy was higher

for the "easy" level. The error bars represent the SEM (standard error of the mean). This figure has been modified from Domic-Siede et al.⁵⁴. [Please click here to view a larger version of this figure.](#)

These results indicated that when the planning component was successfully removed from the control condition (*via* instruction manipulation), the planning task was cognitively more complex, demanding, challenging, and time-consuming. Hence, the neural correlates induced by the tasks could be compared to each other.

To analyze frontal midline theta activity during planning, the average theta frequency band during planning for the Fz electrode was compared to that of the control period, and a significant increase in theta band frequency was found during planning (**Figure 7**).

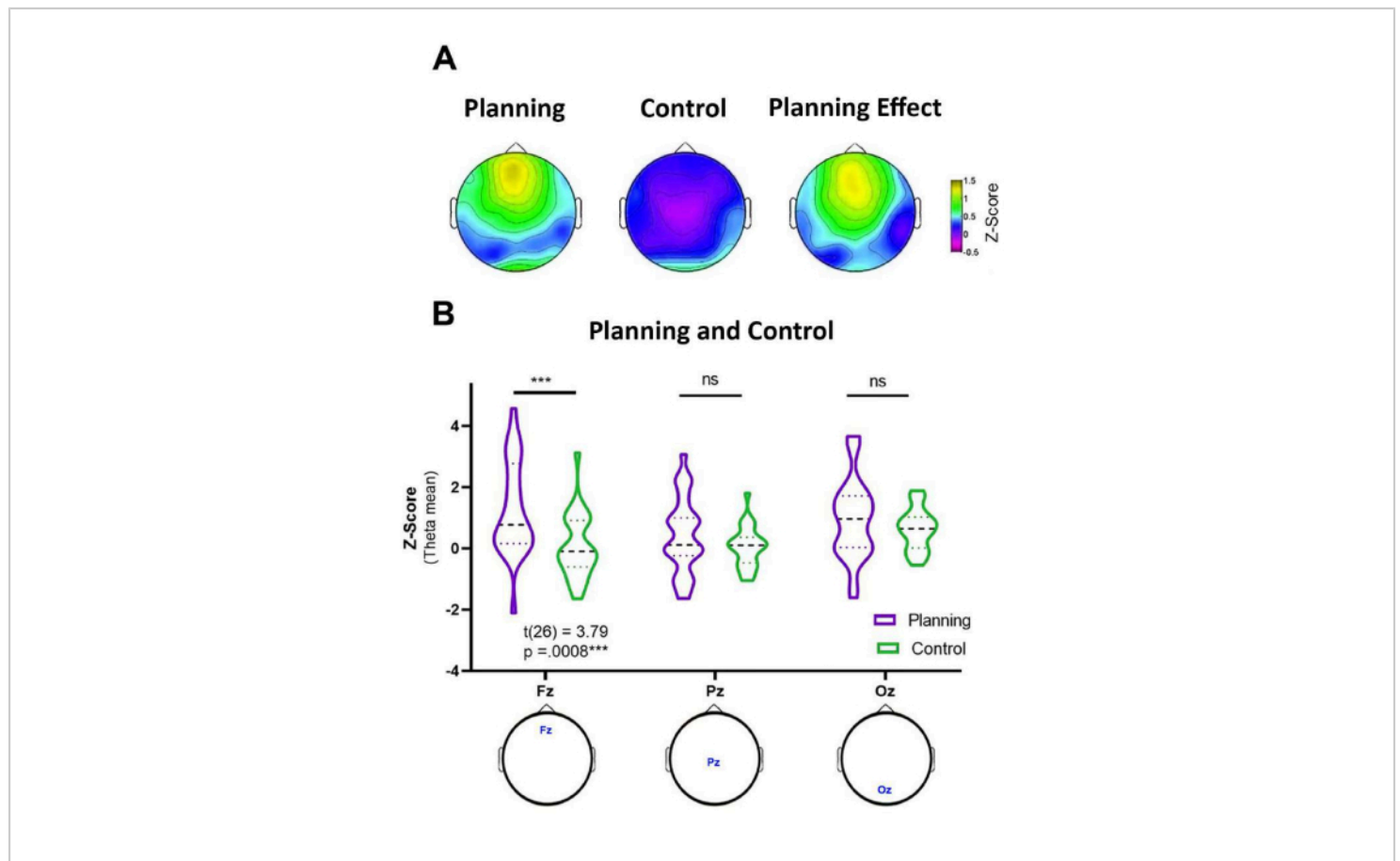


Figure 7: Frontal midline theta activity during cognitive planning. (A) Topographic maps representing the theta band power across all the subjects normalized to the z-scores during the planning task (left), the control task (middle), and the planning effect (right). During cognitive planning, the subjects exhibited an increase in frontal midline theta activity. The color bar shows the z-values between -0.5 to 1.5 . (B) A violin plot showing the minimum, quartiles, median, and maximum z-score values of theta activity across the subjects during planning (purple) compared to the control period (green) for electrodes

Fz (left), Pz (middle), and Oz (right) using a matched-pair t-test. This figure has been modified from Domic-Siede et al.⁵⁴.

[Please click here to view a larger version of this figure.](#)

Additionally, to assess the temporal dynamics of the observed frontal theta activity, topographic maps corresponding to specific time points of theta band power (750 ms, 1,750 ms, 2,750 ms, and 3,750 ms) were formulated (**Figure**

8A). Further, compared to the control period, the time-frequency analysis demonstrated a significant, progressive, and sustained increase in theta activity starting 1 s after the onset of the planning period (**Figure 8B**).

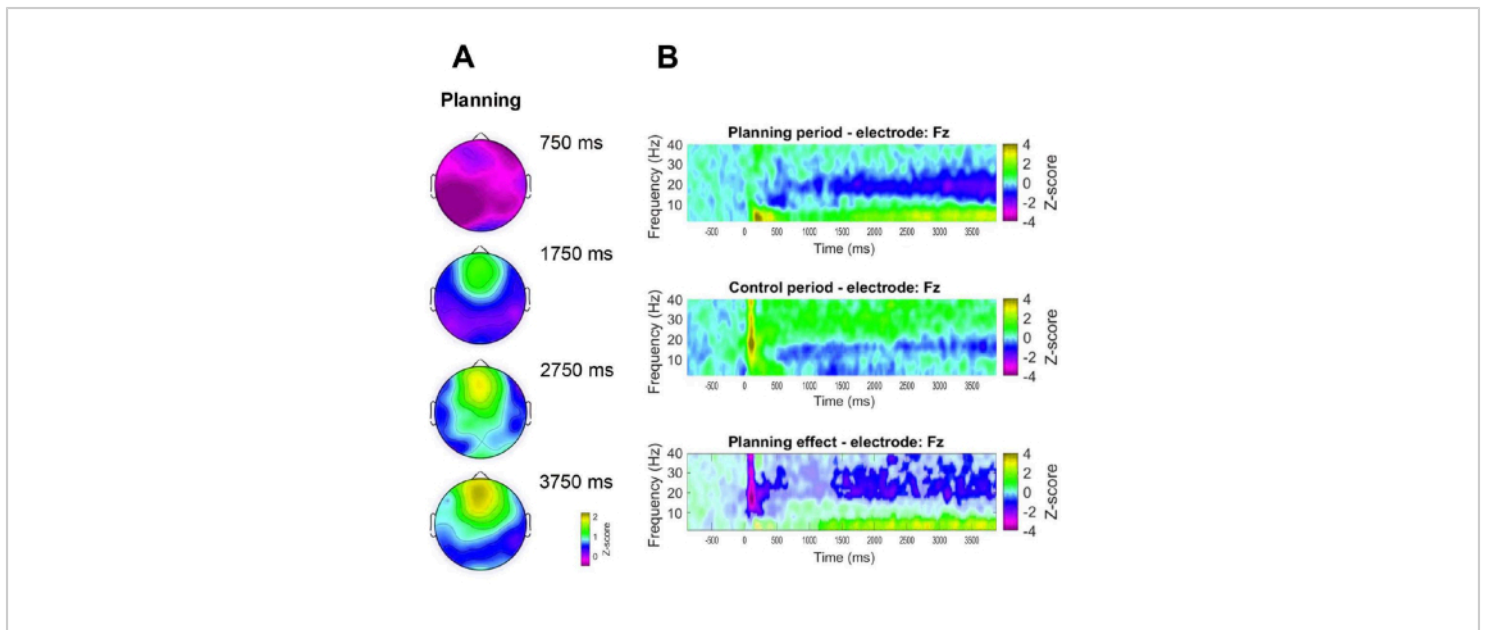


Figure 8: Frontal midline theta temporal dynamics. (A) Topographic time slices of the theta activity. A progressive increase in the frontal midline theta activity across time during planning implementation (planning period) was observed. The color bar indicates the z-score units (−0.5 to 2.2). (B) Time-frequency charts for the planning period (top), the control period (middle), and the planning effect, calculated by subtracting the control period from the planning period (bottom). Non-significant pixels, as determined using a non-parametric cluster-based permutation test for paired samples, are shown lighter in the planning effect plot. The color bar indicates the z-score units (−4 to 4). This figure has been modified from Domic-Siede et al.⁵⁴. [Please click here to view a larger version of this figure.](#)

For source reconstruction of the theta activity, a brain model template was visualized and compared between conditions, and this indicated that the theta activity originated within the prefrontal cortex areas (frontal superior cortex, FS; anterior cingulate cortex, ACC; and mid-cingulate cortex, MCC), as

well as that there were significant differences between the conditions (in the bilateral SF, the bilateral ACC, and the bilateral MCC) (**Figure 9**), with higher theta activity observed in the planning period (**Figure 9**).

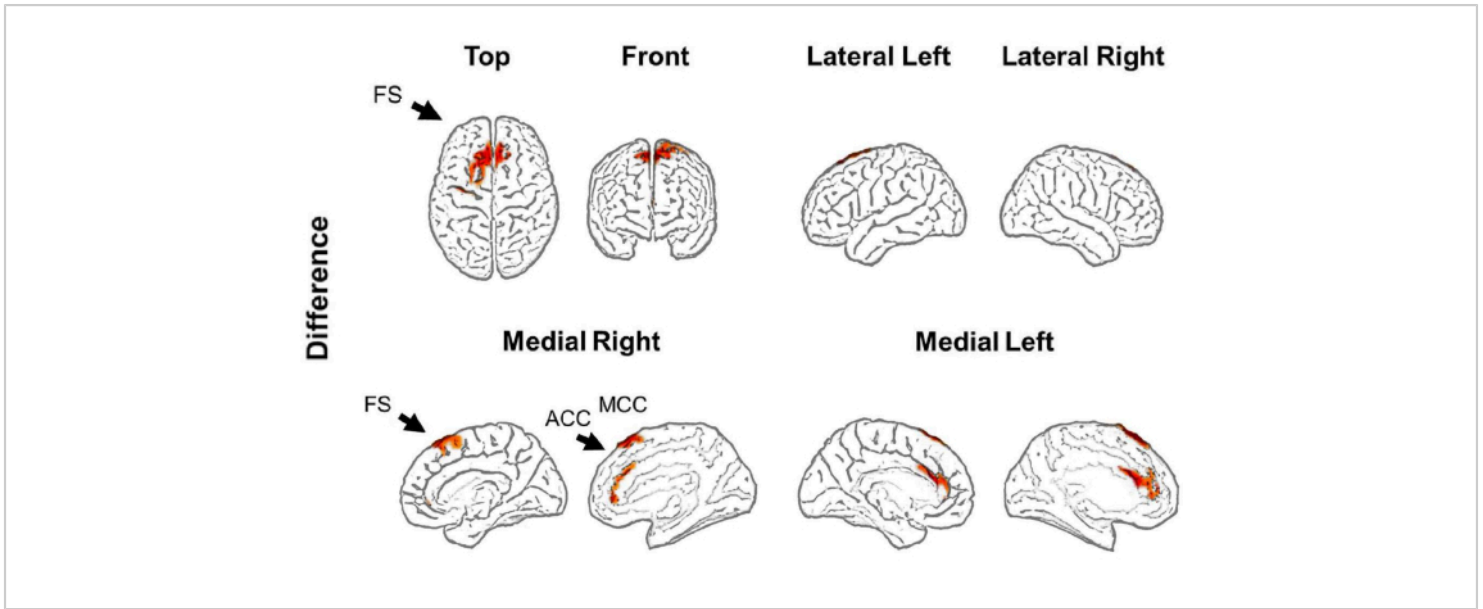


Figure 9: Source reconstruction. An sLORETA algorithm was used to estimate the theta activity from different brain sources. The theta activity was 4-8 Hz bandpass filtered, z-score normalized, corrected by baseline, averaged between 1 s or 4 s after planning or control onset, respectively, and compared between conditions. A significant increase in theta activity was found in the bilateral frontal superior area, the bilateral anterior cingulate cortex, and the bilateral mid-cingulate cortex. The figure shows significant t-values from the permutation test. Abbreviations: FS = frontal superior; ACC = anterior cingulate cortex; MCC = mid-cingulate cortex. This figure has been modified from Domic-Siede et al.⁵⁴. [Please click here to view a larger version of this figure.](#)

Afterward, the time profile of the theta changes over time for each source was evaluated by computing a Hilbert transform, and then we compared the instantaneous amplitude of the theta activity between the conditions. We found that the left frontopolar, bilateral ACC, and bilateral MCC sources

presented higher theta activity after the planning period onset (**Figure 10**). These results suggested that our experimental paradigm demanding cognitive planning induced theta activity originating within the PFC regions.

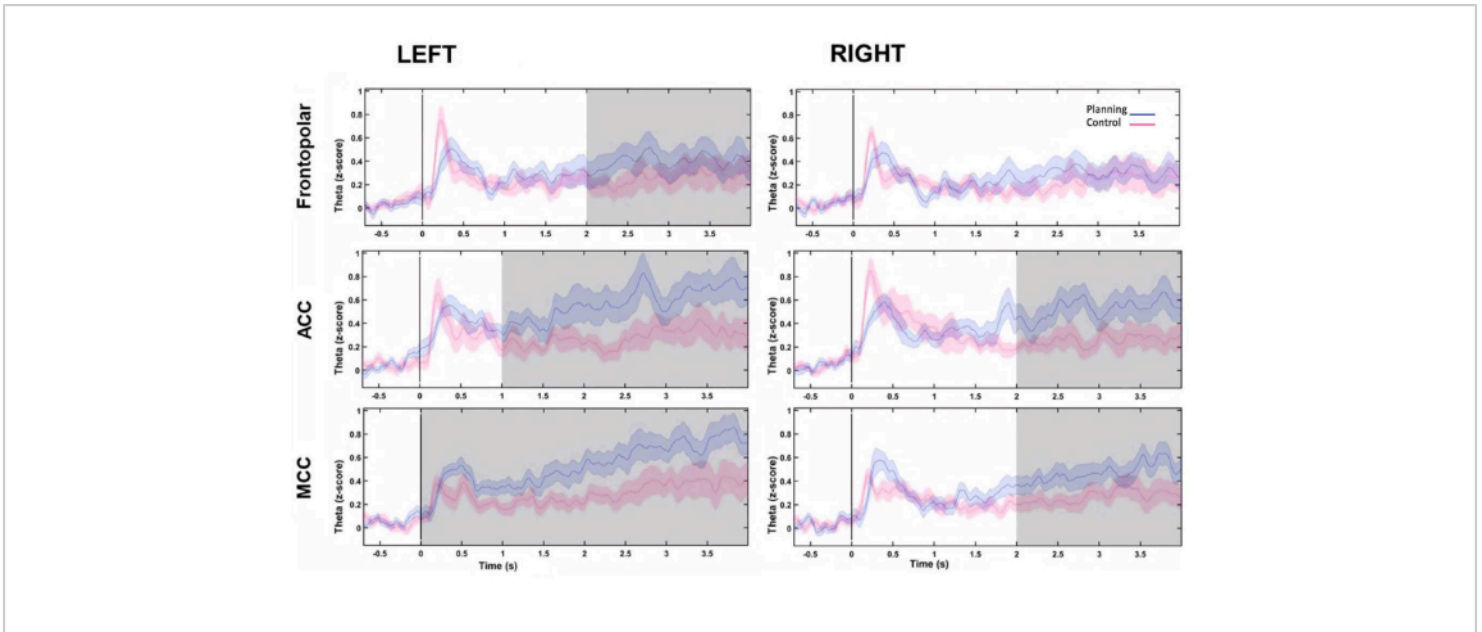


Figure 10: Theta activity time profile of the PFC sources. The instantaneous amplitude calculated with the Hilbert transform was applied to the first component of the PCA decomposition for each frontal source and both conditions and baseline normalized to the z-score to show the frontal theta activity over time. The gray shaded areas show significant differences determined using a non-overlapping moving window with steps of 1 s (Wilcoxon signed-rank test) corrected by the FDR. The shaded regions represent 95% confidence intervals. The left FP region, the bilateral ACC, and the bilateral MCC showed increases in theta activity after planning onset. Abbreviations: ACC = anterior cingulate cortex; MCC = mid-cingulate cortex. The planning condition is shown in purple. The control condition is shown in red. This figure has been modified from Domic-Siede et al.⁵⁴. [Please click here to view a larger version of this figure.](#)

Further, we aimed to examine the variation in spectral features during planning with regard to the complexity level, as indicated by the behavioral results. Of note, a significant discrepancy was found only in the left ACC within the alpha band. This supports the notion that our planning task

evaluates the intrinsic facets of planning through changes in theta oscillations to a greater extent than the general cognitive demands (effort) typically encountered in cognitive control tasks (**Figure 11**).

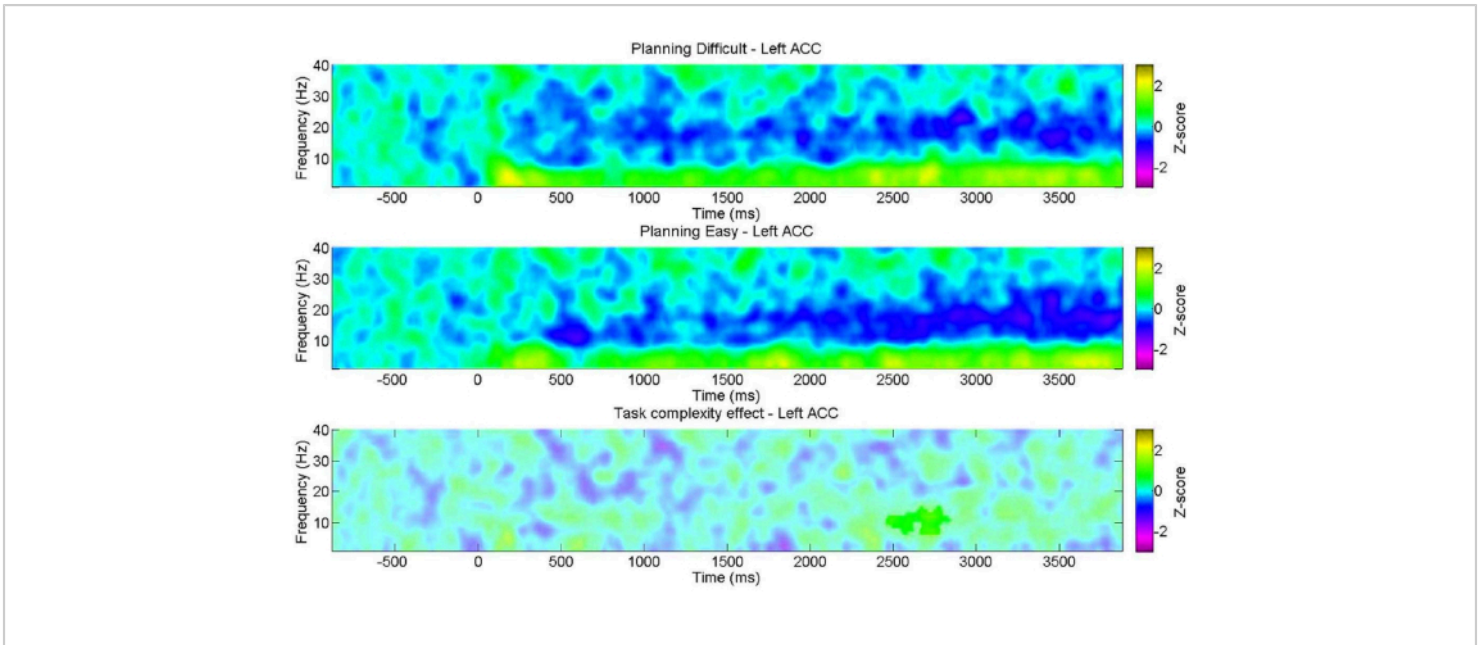


Figure 11: EEG across the planning complexity levels. The ROI time-frequency charts showed a significant positive cluster in the alpha band exclusively in the left anterior cingulate cortex (ACC) for the "difficult" level. Non-significant pixels, as determined using a non-parametric cluster-based permutation test for paired samples, are shown in a lighter shade on the plot, with the color bar indicating the z-score units from -3 to 3 . This figure has been modified from Domic-Siede et al.⁵⁴.

[Please click here to view a larger version of this figure.](#)

When correlations between theta activity and behavioral performance were performed, a negative correlation was observed; specifically, as the theta activity in the left frontopolar region during the planning period increased, the

LISAS planning execution score decreased (**Figure 12**). This pattern may reflect that the left FP region may be necessary during planning elaboration to execute a plan successfully afterward and suggests a role for theta activity.

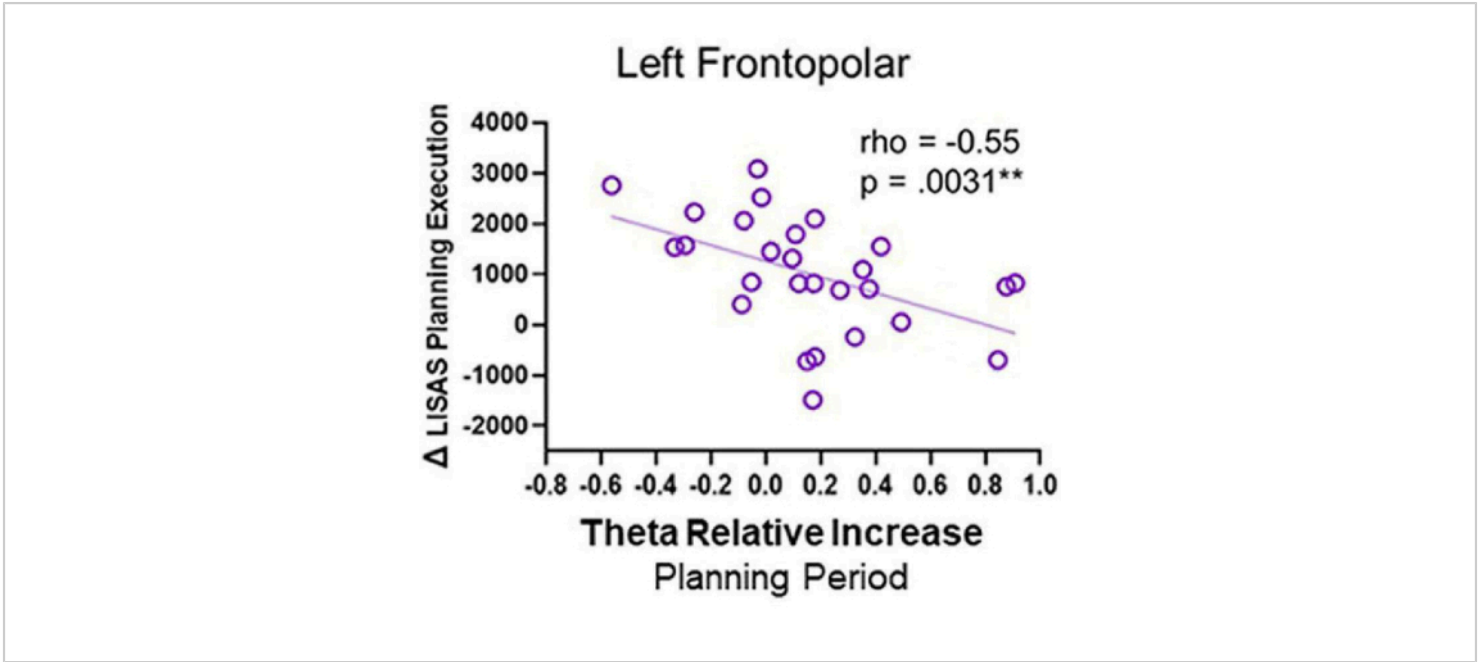


Figure 12: Theta activity and behavioral performance. The Spearman's rho correlation between the theta activity from the left frontopolar cortex and the Δ LISAS planning execution showed a significant negative correlation. This figure has been modified from Domic-Siede et al.⁵⁴. [Please click here to view a larger version of this figure.](#)

Additionally, the varying cognitive demands and goals induced by each condition may have caused contrasting eye movements between the planning and control conditions, leading to differing oscillatory activity patterns⁹⁵. To address

the above issue, we analyzed the single-subject, single-trial data at various levels. Notably, the Fz channel time series and theta activity time dynamics appeared to have no connection with the rate of saccades over time (**Figure 13A**).

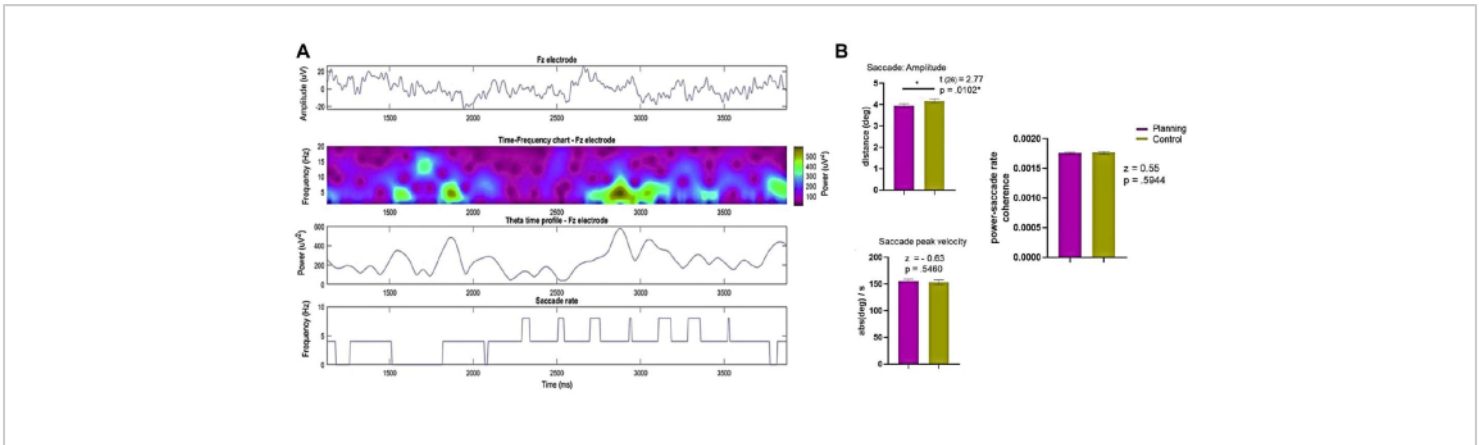


Figure 13: Results of EEG and eye movement recordings. (A) The rows present the EEG (top), the time-frequency chart (middle top), the theta time profile from electrode Fz (middle bottom), and the saccade rate of subject 8 and trial 9 (bottom) in the planning condition. (B) A Wilcoxon signed-rank test comparison of the saccade amplitude, saccade peak velocity, and power-saccade rate coherence between the conditions is shown, revealing significant statistical differences in the saccade amplitude between the planning and control conditions. The SEM is represented by the error bars. This figure has been modified from Domic-Siede et al.⁵⁴. [Please click here to view a larger version of this figure.](#)

Next, we obtained the saccade amplitude and peak velocity from the entire trial and from 0 s to 3.75 s for comparison (Figure 13B). We discovered that the saccade amplitude was larger in the control condition. However, no statistically significant differences were found between the conditions in the coherence index between the Fourier theta power at electrode Fz and the saccade rate (Figure 10B), indicating that any potential relationship between saccades and theta activity was consistent across conditions.

Taken together, these results support that the experimental protocol described is suitable for studying cognitive planning as a cognitive control function.

Discussion

The protocol described here offers an innovative approach for assessing cognitive planning and cognitive control during a novel and ecological planning task in association with pertinent and complementary behavioral and physiological measurements, such as oscillatory and pupillary dynamics. During our experiments, EEG activity was recorded while the participants performed the planning task, in which the participants were instructed to first elaborate and then execute a plan. The control condition, which involved evaluating a pre-drawn path on the zoo map, was established to eliminate the cognitive planning aspect while maintaining a similar setting and structure. This approach enables the assessment of whether cognitive planning, as a cognitive control function, leads to the generation of frontal theta

activity from PFC regions and whether different PFC theta oscillation sources are linked to different aspects of planning performance. Another aspect that might be evaluated using this protocol is the differentiation of the various cognitive processes involved during phases of planning, such as plan elaboration, plan execution, plan achievement, and feedback processing. We found that planning induced a canonical frontal theta activity associated with cognitive control, which contributed to efficiently achieving a goal. These results underpin the interest of this protocol.

Despite the vast developments in cognitive neuroscience, most neuroimaging experiments examine isolated cognitive functions using artificial tasks in sensorimotor-deprived environments and oversimplified stimuli to control confounds. Problematically, those experiments might not be able to identify the real brain mechanisms involved when a cognitive function is implemented in an everyday situation (during ecological situations)^{138,140}. In particular, the capacities for formulating goals, planning, and executing plans effectively are difficult to assess since they require various cognitive functions (working memory, inhibitory control, cognitive flexibility, etc.)^{104,144}. Thus, designing an ecological behavioral task is encouraged and suggested based on the current trends in cognitive neuroscience^{142,143,145,146}.

Our planning task, despite taking place in a laboratory environment (inside a room with the stimuli displayed on a screen), was made engaging and interactive for participants

through the use of meaningful stimuli and goals that they could interact with on the screen. Additionally, the task requires participants to engage in a real-life situation-planning a path to visit various locations. To have an ecological task design, the paradigm must challenge the subjects to perform a specific behavior or cognitive function in a manner similar to what they would have to do in everyday life^{62,63,147}. To develop an ecological task design, the planning task used here involves planning a path to visit different places in several stages⁵⁶. The first stage involves the participants creating a plan while ensuring it follows a set of rules. The second stage involves maintaining the plan in working memory, while the third stage involves executing the plan and monitoring its adherence to the rules. These stages represent different phases of planning and the orchestration of other executive functions, such as cognitive flexibility, inhibitory control, and working memory. In order to have a valid ecological cognitive task design, the task should be able to detect specific cognitive impairments in patients with psychiatric or cognitive disorders who have difficulty performing that specific cognitive function in their daily life¹⁰⁵. This can be achieved through future research using this protocol.

The behavioral results obtained through the use of this protocol were aligned with the experimental predictions. A significant difference in behavior was observed when the planning component was removed from the control task to form a control condition, thus facilitating further comparisons. The planning condition was found to be cognitively more demanding than the control condition, as evidenced by parameters such as the reaction time and accuracy. This may reflect the increased involvement of high cognitive functions in the implementation of planning^{23,55,56,57,148,149,150}.

Considering that the control condition involved less complex cognition, as evidenced by the faster reaction times, better performances, and different cognitive processes required (the evaluation of rules), a possible alternative modification is to exploit the complexity levels present in the planning task, manipulate them, and analyze the planning function parametrically according to different levels of complexity (for instance, increasing the number of trials, and creating difficult, medium, and easy trial conditions). However, the results from our protocol showed that while it was possible to distinguish between "easy" and "difficult" trials based on behavioral measures, there were no differences detected in electrophysiological measures. This suggests that the results in our protocol more accurately reflect the intrinsic characteristics of the planning function rather than broader aspects of cognitive control, such as attention, mental effort, level of difficulty, or a high level of cognitive demand⁵⁴. Nevertheless, further research may consider other types of control conditions, such as following a marked path that visits the four animal locations but also remembering the sequence order. This way, the level of difficulty could be better controlled, and planning could be distinguished from working memory, but one possible disadvantage of this is fatigue, because the subjects would have to perform two highly demanding tasks.

Several studies have linked different eye movement parameters with specific cognitive events. On the one hand, certain studies have found correlations between theta oscillations and pupil diameter during cognitive tasks, suggesting a relationship between these two measures of cognitive function. For example, Lin et al.¹⁵² found a correlation between midfrontal theta activity and changes in pupil size, reflecting varying degrees of subjective conflict. Their findings suggest that these signals represent conflict

processing, increased attention, and flexible behavioral responses. Hence, the relationship between midfrontal theta activity and pupil responses seems to play a role in weighing costs and benefits during decision-making processes. In another study, Yu et al.¹⁵³ examined how time-on-task engagement neurophysiologically affects cognitive control through a working memory task that modulated control inhibitory responses. They studied the relationship between pupil diameter data and frontal theta activity and showed that as the task duration increased, the performance decreased, and this was accompanied by a decrease in pupil dilation modulation and frontal theta activity. At the beginning of the task, they found a strong correlation between task engagement, theta activity, and cognitive control, as indicated by pupil dilation modulation, principally for demanding tasks that required high working memory and inhibitory control. However, this relationship dissipated toward the end, signaling a disconnection between the effort invested and the cognitive control used for performing the task, which is a hallmark of prefrontal time-on-task effects¹⁵³. On the other hand, other studies have investigated saccades and oscillations. For example, Nakatani et al.¹⁵⁴ revealed that, in a perceptual task, the alpha band amplitude from occipital regions predicted blinks and saccade effects. Moreover, Velasques et al.¹⁵⁵ showed that, during a prosaccadic attention task, the saccade amplitude was associated with frontal gamma changes. Furthermore, Bodala et al.¹⁵⁶ found that decreases in frontal midline theta were accompanied by decreases in sustained attention, as well as the amplitude and velocity of saccades. These findings suggest that eye movements, especially saccades, may reflect cognitive processes rather than just contributing to the background noise in EEG signals. In the current study, we enhanced the elimination of eye movement-related artifacts using the ICA algorithm with the saccade-to-fixation variance ratio

criterion¹²⁶. This criterion enhances artifact removal for free viewing tasks¹⁵⁷. In our study, no differences were observed in saccade peak velocity and the coherence between theta power and saccade rate across conditions. However, more studies are needed to address these questions.

A critical step in using this protocol is constantly calibrating the eye tracker during the experiment, as the loss of gaze data from the camera could result in errors that would contaminate the task and make it difficult to obtain accurate responses. Therefore, it is crucial to calibrate as often as possible. However, there is a trade-off between the number of trials with a calibrated eye tracker and the length of the experiment. In our study, we decided to calibrate every five trials.

Future research exploring the relationship between theta oscillations and pupil diameter during this planning task should be conducted. Planning is a critical aspect of executive control that requires the allocation of attentional resources and the coordination of multiple cognitive processes. Understanding the relationship between theta oscillations and pupil diameter during planning tasks could provide valuable insights into the underlying neural mechanisms of executive control and how they change over time. Furthermore, such studies could lead to a deeper understanding of how changes in cognitive function, such as fatigue or attentional lapses, affect performance on planning tasks and the ability to allocate resources effectively. This information could have important implications for developing interventions aimed at improving planning performance, such as cognitive training programs or treatments for conditions such as attention-deficit/hyperactivity disorder (ADHD), among others.

Previous research has indicated that the PFC plays a crucial role in cognitive planning, as confirmed by our results. These results demonstrate that cognitive planning induces FM0

activity in the PFC, particularly in the anterior cingulate cortex, mid-cingulate cortex, and superior frontal regions⁵⁴. These findings align with prior research on executive functions. There is substantial evidence to support the idea that FM θ activity acts as a top-down process for initiating control and facilitating communication between brain regions during demanding tasks¹³. While only a few studies have examined the temporal dynamics of FM θ activity associated with cognitive control, there is widespread agreement that the time profile of FM θ can provide information about various facets of cognitive control and the involvement of distinct PFC regions. Using our protocol for evaluating cognitive planning allowed us to characterize the time profile of FM θ activity during planning. Specifically, the FM θ activity during the planning condition showed a progressive increase. By implementing this protocol, for the first time, it was demonstrated that FM θ is also present during planning implementation, as in other higher-order cognitive functions, and its temporal dynamics may serve as an indicator of cognitive control.

Our results and protocol have potential applications in the field of neuroscience, including for improving virtual neuropsychological assessments and the treatment of neuropsychiatric disorders with associated cognitive planning issues, such as depression and attention-deficit/hyperactivity disorder. For example, assessments could involve examining different patterns of errors at the behavioral performance level, different oscillatory patterns at the electrophysiological level, and different eye movements. Additionally, the results of this work may inform the development of brain-computer interfaces and cognitive training programs that aim to enhance cognitive planning abilities.

The present protocol may contribute new evidence to understanding the neural mechanisms that underpin the

elusive cognitive control function of cognitive planning in neurotypical and neuropsychiatric populations. Moreover, our behavioral paradigm might offer insights into the neurobiology of cognitive control and planning through the examination of electrophysiological, pupillometry, and behavioral measurements with a practical planning task that examines intrinsic aspects of planning rather than the general cognitive demands typically present in cognitive control tasks, as reflected in the changes in theta oscillations.

Disclosures

The authors have nothing to disclose.

Acknowledgments

This research was financially supported by the doctoral scholarship program Becas de Doctorado Nacional año 2015 of ANID 21150295, FONDECYT regular grant 1180932, FONDECYT regular grant 1230383, FONDECYT de Iniciación grant 11220009, Postdoc grant Universidad de O'Higgins, and the Institut Universitaire de France (IUF). We want to thank Professor Pablo Billeke for his feedback on the paradigm design. We thank Professor Eugenio Rodríguez for kindly sharing his time-frequency analysis codes. Finally, we thank Milan Domic, Vicente Medel, Josefina Ihnen, Andrea Sánchez, Gonzalo Boncompte, Catalina Fabar, and Daniela Santander for their feedback.

References

1. Siegel, M., Donner, T. H., Engel, A. K. Spectral fingerprints of large-scale neuronal interactions. *Nature Reviews Neuroscience*. **13** (2), 121-134 (2012).
2. Fries, P. A mechanism for cognitive dynamics: Neuronal communication through neuronal coherence. *Trends in Cognitive Sciences*. **9** (10), 474-480 (2005).

3. Fries, P. Rhythms for cognition: Communication through coherence. *Neuron*. **88** (1), 220-235 (2015).
4. Thut, G., Miniussi, C., Gross, J. The functional importance of rhythmic activity in the brain. *Current Biology*. **22** (16), R658-R663 (2012).
5. Fröhlich, F., McCormick, D. A. Endogenous electric fields may guide neocortical network activity. *Neuron*. **67** (1), 129-143 (2010).
6. Spaak, E., de Lange, F. P., Jensen, O. Local entrainment of alpha oscillations by visual stimuli causes cyclic modulation of perception. *Journal of Neuroscience*. **34** (10), 3536-3544 (2014).
7. Fiebelkorn, I. C., Saalman, Y. B., Kastner, S. Rhythmic sampling within and between objects despite sustained attention at a cued location. *Current Biology*. **23** (24), 2553-2558 (2013).
8. Landau, A. N., Fries, P. Attention samples stimuli rhythmically. *Current Biology*. **22** (11), 1000-1004 (2012).
9. Song, K., Meng, M., Lin, C., Zhou, K., Luo, H. Behavioral oscillations in attention: Rhythmic α pulses mediated through θ band. *Journal of Neuroscience*. **34** (14), 4837-4844 (2014).
10. Wyart, V., Nobre, A. C., Summerfield, C. Dissociable prior influences of signal probability and relevance on visual contrast sensitivity. *Proceedings of the National Academy of Sciences of the United States of America*. **109** (9), 3593-3598 (2012).
11. Leszczyński, M., Fell, J., Axmacher, N. Rhythmic working memory activation in the human hippocampus. *Cell Reports*. **13** (6), 1272-1282 (2015).
12. Onton, J., Delorme, A., Makeig, S. Frontal midline EEG dynamics during working memory. *NeuroImage*. **27** (2), 341-356 (2005).
13. Cavanagh, J. F., Frank, M. J. Frontal theta as a mechanism for cognitive control. *Trends in Cognitive Sciences*. **18** (8), 414-421 (2014).
14. Siegel, M., Buschman, T. J., Miller, E. K. Cortical information flow during flexible sensorimotor decisions. *Science*. **348** (6241), 1352-1355 (2015).
15. Weisz, N. et al. Prestimulus oscillatory power and connectivity patterns predispose conscious somatosensory perception. *Proceedings of the National Academy of Sciences of the United States of America*. **111** (4), E417-E425 (2014).
16. Buzsáki, G., Draguhn, A. Neuronal oscillations in cortical networks. *Science*. **304** (5679), 1926-1929 (2004).
17. Cohen, M. X. A neural microcircuit for cognitive conflict detection and signaling. *Trends in Neurosciences*. **37** (9), 480-490 (2014).
18. Yuste, R. From the neuron doctrine to neural networks. *Nature Reviews Neuroscience*. **16** (8), 487-497 (2015).
19. Helfrich, R. F., Knight, R. T. Oscillatory dynamics of prefrontal cognitive control. *Trends in Cognitive Sciences*. **20** (12), 916-930 (2016).
20. Miller, E. K., Cohen, J. D. An integrative theory of prefrontal cortex function. *Annual Review of Neurosciences*. **24** (1), 167-202 (2001).
21. von Nicolai, C. et al. Corticostriatal coordination through coherent phase-amplitude coupling. *Journal of Neuroscience*. **34** (17), 5938-5948 (2014).
22. Sweeney-Reed, C. M. et al. Thalamic theta phase alignment predicts human memory formation and

- anterior thalamic cross-frequency coupling. *ELife*. **4**, e07578 (2015).
23. Voytek, B. et al. Oscillatory dynamics coordinating human frontal networks in support of goal maintenance. *Nature Neuroscience*. **18** (9), 1318-1324 (2015).
 24. Raghavachari, S. et al. Theta oscillations in human cortex during a working-memory task: Evidence for local generators. *Journal of Neurophysiology*. **95** (3), 1630-1638 (2006).
 25. Jacobs, J., Hwang, G., Curran, T., Kahana, M. J. EEG oscillations and recognition memory: Theta correlates of memory retrieval and decision making. *NeuroImage*. **32** (2), 978-987 (2006).
 26. Itthipuripat, S., Wessel, J. R., Aron, A. R. Frontal theta is a signature of successful working memory manipulation. *Experimental Brain Research*. **224** (2), 255-262 (2013).
 27. Cavanagh, J. F., Zambrano-Vazquez, L., Allen, J. J. B. Theta lingua franca: A common mid-frontal substrate for action monitoring processes. *Psychophysiology*. **49** (2), 220-238 (2012).
 28. Mas-Herrero, E., Marco-Pallarés, J. Frontal theta oscillatory activity is a common mechanism for the computation of unexpected outcomes and learning rate. *Journal of Cognitive Neuroscience*. **26** (3), 447-458 (2014).
 29. Folstein, J. R., Van Petten, C. Influence of cognitive control and mismatch on the N2 component of the ERP: A review. *Psychophysiology*. **45** (1), 152-170 (2008).
 30. Cohen, M. X., Donner, T. H. Midfrontal conflict-related theta-band power reflects neural oscillations that predict behavior. *Journal of Neurophysiology*. **110** (12), 2752-2263 (2013).
 31. Walsh, M. M., Anderson, J. R. Modulation of the feedback-related negativity by instruction and experience. *Proceedings of the National Academy of Sciences of the United States of America*. **108** (47), 19048-19053 (2011).
 32. Luu, P., Tucker, D. M., Makeig, S. Frontal midline theta and the error-related negativity: Neurophysiological mechanisms of action regulation. *Clinical Neurophysiology*. **115** (8), 1821-1835 (2004).
 33. Hanslmayr, S. et al. The electrophysiological dynamics of interference during the Stroop task. *Journal of Cognitive Neuroscience*. **20** (2), 215-225 (2008).
 34. Cavanagh, J. F., Cohen, M. X., Allen, J. J. B. Prelude to and resolution of an error: EEG phase synchrony reveals cognitive control dynamics during action monitoring. *Journal of Neuroscience*. **29** (1), 98-105 (2009).
 35. Cohen, M. X., van Gaal, S., Ridderinkhof, K. R., Lamme, V. A. F. Unconscious errors enhance prefrontal-occipital oscillatory synchrony. *Frontiers in Human Neuroscience*. **3**, 54 (2009).
 36. Cavanagh, J. F., Frank, M. J., Klein, T. J., Allen, J. J. B. Frontal theta links prediction errors to behavioral adaptation in reinforcement learning. *NeuroImage*. **49** (4), 3198-3209 (2010).
 37. Cohen, M. X., Cavanagh, J. F. Single-trial regression elucidates the role of prefrontal theta oscillations in response conflict. *Frontiers in Psychology*. **2**, 30 (2011).
 38. Cohen, M. X., Van Gaal, S. Dynamic interactions between large-scale brain networks predict behavioral adaptation after perceptual errors. *Cerebral Cortex*. **23** (5), 1061-1072 (2013).

39. Nigbur, R., Cohen, M. X., Ridderinkhof, K. R., Stürmer, B. Theta dynamics reveal domain-specific control over stimulus and response conflict. *Journal of Cognitive Neuroscience*. **24** (5), 1264-1274 (2012).
40. van Driel, J., Swart, J. C., Egnér, T., Ridderinkhof, K. R., Cohen, M. X. (No) time for control: Frontal theta dynamics reveal the cost of temporally guided conflict anticipation. *Cognitive, Affective, and Behavioral Neuroscience*. **15** (4), 787-807 (2015).
41. van de Vijver, I., Ridderinkhof, K. R., Cohen, M. X. Frontal oscillatory dynamics predict feedback learning and action adjustment. *Journal of Cognitive Neuroscience*. **23** (12), 4106-4121 (2011).
42. Narayanan, N. S., Cavanagh, J. F., Frank, M. J., Laubach, M. Common medial frontal mechanisms of adaptive control in humans and rodents. *Nature Neuroscience*. **16** (12), 1888-1895 (2013).
43. Anguera, J. A. et al. Video game training enhances cognitive control in older adults. *Nature*. **501** (7465), 97-101 (2013).
44. Smit, A. S., Eling, P. A. T. M., Hopman, M. T., Coenen, A. M. L. Mental and physical effort affect vigilance differently. *International Journal of Psychophysiology*. **57** (3), 211-217 (2005).
45. Cohen, M. X., Ranganath, C. Reinforcement learning signals predict future decisions. *Journal of Neuroscience*. **27** (2), 371-378 (2007).
46. Gehring, W. J., Goss, B., Coles, M. G. H., Meyer, D. E., Donchin, E. A neural system for error detection and compensation. *Psychological Science*. **4** (6), 385-390 (1993).
47. Yeung, N., Botvinick, M. M., Cohen, J. D. The neural basis of error detection: Conflict monitoring and the error-related negativity. *Psychological Review*. **111** (4), 931-959 (2004).
48. Debener, S. et al. Trial-by-trial coupling of concurrent electroencephalogram and functional magnetic resonance imaging identifies the dynamics of performance monitoring. *Journal of Neuroscience*. **25** (50), 11730-11737 (2005).
49. Hauser, T. U. et al. The feedback-related negativity (FRN) revisited: New insights into the localization, meaning, and network organization. *NeuroImage*. **84**, 159-168 (2014).
50. Wang, C., Ulbert, I., Schomer, D. L., Marinkovic, K., Halgren, E. Responses of human anterior cingulate cortex microdomains to error detection, conflict monitoring, stimulus-response mapping, familiarity, and orienting. *Journal of Neuroscience*. **25** (3), 604-613 (2005).
51. Tsujimoto, S., Genovesio, A. Firing variability of frontal pole neurons during a cued strategy task. *Journal of Cognitive Neuroscience*. **29** (1), 25-36 (2017).
52. Womelsdorf, T., Johnston, K., Vinck, M., Everling, S. Theta-activity in anterior cingulate cortex predicts task rules and their adjustments following errors. *Proceedings of the National Academy of Sciences of the United States of America*. **107** (11), 5248-5253 (2010).
53. Womelsdorf, T., Vinck, M., Stan Leung, L., Everling, S. Selective theta synchronization of choice-relevant information subserves goal-directed behavior. *Frontiers in Human Neuroscience*. **4**, 210 (2010).

54. Domic-Siede, M., Irani, M., Valdés, J., Perrone-Bertolotti, M., Ossandón, T. Theta activity from frontopolar cortex, mid-cingulate cortex and anterior cingulate cortex shows different roles in cognitive planning performance. *NeuroImage*. **226**, 117557 (2021).
55. Wilensky, R. *Planning and Understanding: A Computational Approach to Human Reasoning*. Addison-Wesley. Reading, MA (1983).
56. Grafman, J., Hendler, J. Planning and the brain. *Behavioral and Brain Sciences*. **14**, 563-564. (1991).
57. Hayes-Roth, B., Hayes-Roth, F. A cognitive model of planning. *Cognitive Science*. **3** (4), 275-310 (1979).
58. Tremblay, M. et al. Brain activation with a maze test: An EEG coherence analysis study in healthy subjects. *Neuroreport*. **5** (18), 2449-2453 (1994).
59. Shallice, T. Specific impairments of planning. *Philosophical Transactions of the Royal Society B: Biological Sciences*. **298** (1089), 199-209 (1982).
60. Unterrainer, J. M., Owen, A. M. Planning and problem solving: From neuropsychology to functional neuroimaging. *Journal of Physiology*. **99** (4-6), 308-317 (2006).
61. Domic-Siede, M. et al. La planificación cognitiva en el contexto de la evaluación neuropsicológica e investigación en neurociencia cognitiva: Una revisión sistemática. *Terapia Psicológica*. **40** (3), 367-395 (2022).
62. Miotto, E. C., Morris, R. G. Virtual planning in patients with frontal lobe lesions. *Cortex*. **34** (5), 639-657 (1998).
63. Burgess, P. W., Simons, J. S., Coates, L. M. A., Channon, S. The search for specific planning processes. In *The Cognitive Psychology of Planning*, edited by Morris, R., Ward, G., 199-227. Psychology Press. Hove, UK (2005).
64. Oosterman, J. M., Wijers, M., Kessels, R. P. C. Planning or something else? Examining neuropsychological predictors of zoo map performance. *Applied Neuropsychology*. **20** (2), 103-109 (2013).
65. Campbell, Z. et al. Utilizing virtual reality to improve the ecological validity of clinical neuropsychology: An fMRI case study elucidating the neural basis of planning by comparing the Tower of London with a three-dimensional navigation task. *Applied Neuropsychology*. **16** (4), 295-306 (2009).
66. Wilson, B. A., Alderman, N., Burgess, P. W., Emslie, H., Evans, J. J. *Behavioural Assessment of the Dysexecutive Syndrome*. Thames Valley Test Company. St Edmunds, UK (1996).
67. Spector, L., Grafman, J. Planning, neuropsychology, and artificial intelligence: Cross fertilization. In *Handbook of Neuropsychology*, edited by Boller, F., Grafman, J., volume 9, 377-392. Elsevier Science Publishers. Amsterdam, the Netherlands (1994).
68. Porteus, S. D. *The Maze Test and Clinical Psychology*. Pacific Books. Palo Alto, California (1959).
69. Lis, S., Krieger, S., Wilhelm, J., Gallhofer, B. Feedback about previous action improves executive functioning in schizophrenia: An analysis of maze solving behaviour. *Schizophrenia Research*. **78** (2-3), 243-250 (2005).
70. Zelinsky G. J. A theory of eye movements during target acquisition. *Psychological Review*. **115** (4), 787-835 (2008).

71. Wurtz, R. H., Goldberg, M. E., Robinson, D. L. Brain mechanisms of visual attention. *Scientific American*. **246** (6), 124-135 (1982).
72. Burr, D., Morrone, M. C. Eye movements: Building a stable world from glance to glance. *Current Biology*. **15** (20), R839-R840 (2005).
73. Rolfs M. Microsaccades: Small steps on a long way. *Vision Research*. **49** (20), 2415-2441 (2009).
74. Ortega, J., Plaska, C. R., Gomes, B. A., Ellmore, T. M. Spontaneous eye blink rate during the working memory delay period predicts task accuracy. *Frontiers in Psychology*. **13**, 788231 (2022).
75. Grueschow, M., Kleim, B., Ruff, C. C. Role of the locus coeruleus arousal system in cognitive control. *Journal of Neuroendocrinology*. **32** (12), e12890 (2020).
76. Aston-Jones, G., Shaver, R., Dinan, T. Cortically projecting nucleus basalis neurons in rat are physiologically heterogeneous. *Neuroscience Letters*. **46** (1), 19-24 (1984).
77. Foote, S. L., Bloom, F. E., Aston-Jones, G. Nucleus locus coeruleus: New evidence of anatomical and physiological specificity. *Physiological Reviews*. **63** (3), 844-914 (1983).
78. Siever, L. J., Davis, K. L. Overview: Toward a dysregulation hypothesis of depression. *The American Journal of Psychiatry*. **142** (9), 1017-1031 (1985).
79. Aston-Jones, G., Gold, J.I. How we say no: Norepinephrine, inferior frontal gyrus, and response inhibition. *Biological Psychiatry*. **65** (7), 548-549 (2009).
80. Aston-Jones, G., Cohen, J. D. An integrative theory of locus coeruleus norepinephrine function: adaptive gain and optimal performance. *Annual Review of Neurosciences*. **28**, 403-450 (2005).
81. Einhauser, W., Stout, J., Koch, C., Carter, O. Pupil dilation reflects perceptual selection and predicts subsequent stability in perceptual rivalry. *Proceedings of the National Academy of Sciences of the United States of America*. **105** (5), 1704-1709 (2008).
82. Yoshitomi, T., Ito, Y., Inomata, H. Adrenergic excitatory and cholinergic inhibitory innervations in the human iris dilator. *Experimental Eye Research*. **40** (3), 453-459 (1985).
83. Rajkowski, J., Kubiak, P., Aston-Jones, G. Locus coeruleus activity in monkey: Phasic and tonic changes are associated with altered vigilance. *Brain Research Bulletin*. **35** (5-6), 607-616 (1994).
84. Beatty, J. Task-evoked pupillary responses, processing load, and the structure of processing resources. *Psychological Bulletin*. **91** (2), 276-292 (1982).
85. Beatty, J., Kahneman, D. Pupillary changes in two memory tasks. *Psychonomic Science*. **5**, 371-372 (1966).
86. Hess, E. H., Polt, J. M. Pupil size in relation to mental activity during simple problem-solving. *Science*. **143** (3611), 1190-1192 (1964).
87. Kuchinke, L., Vo, M. L., Hofmann, M., Jacobs, A. M. Pupillary responses during lexical decisions vary with word frequency but not emotional valence. *International Journal of Psychophysiology*. **65** (2), 132-140 (2007).
88. Barkley, R. A. Adolescents with attention-deficit/hyperactivity disorder: An overview of empirically based treatments. *Journal of Psychiatric Practice*. **10** (1), 39-56 (2004).

89. Gau, S. S. F., Shang, C. Y. Executive functions as endophenotypes in ADHD: Evidence from the Cambridge Neuropsychological Test Battery (CANTAB). *Journal of Child Psychology and Psychiatry and Allied Disciplines*. **51** (7), 838-849 (2010).
90. Bora, E., Harrison, B. J., Yücel, M., Pantelis, C. Cognitive impairment in euthymic major depressive disorder: A meta-analysis. *Psychological Medicine*. **43** (10), 2017-2026 (2013).
91. Rive, M. M., Koeter, M. W. J., Veltman, D. J., Schene, A. H., Ruhé, H. G. Visuospatial planning in unmedicated major depressive disorder and bipolar disorder: Distinct and common neural correlates. *Psychological Medicine*. **46** (11), 2313-2328 (2016).
92. Holt, D. V., Wolf, J., Funke, J., Weisbrod, M., Kaiser, S. Planning impairments in schizophrenia: Specificity, task independence and functional relevance. *Schizophrenia Research*. **149** (1-13), 174-179 (2013).
93. Lima-Silva, T. B. et al. Functional profile of patients with behavioral variant frontotemporal dementia (bvFTD) compared to patients with Alzheimer's disease and normal controls. *Dementia and Neuropsychologia*. **7** (1), 96-103 (2013).
94. Karnath, H. O., Wallesch, C. W., Zimmermann, P. Mental planning and anticipatory processes with acute and chronic frontal lobe lesions: A comparison of maze performance in routine and non-routine situations. *Neuropsychologia*. **29** (4), 271-290 (1991).
95. Staudigl, T., Hartl, E., Noachtar, S., Doeller, C. F., Jensen, O. Saccades are phase-locked to alpha oscillations in the occipital and medial temporal lobe during successful memory encoding. *PLoS Biology*. **15** (12), e2003404 (2017).
96. Faul, F., Erdfelder, E., Lang, A. G., Buchner, A. G*Power 3: A flexible statistical power analysis program for the social, behavioral, and biomedical sciences. *Behavior Research Methods*. **39** (2), 175-191 (2007).
97. Ferrando, L., Bobes, J., Gibert, J., Soto, M. MINI Entrevista Neuropsiquiátrica Internacional (MINI International Neuropsychiatric Interview, MINI). *Instrumentos de Detección y Orientación Diagnóstica*. Retrieved from <www.novartis.es> (2000).
98. McAssey, M., Dowsett, J., Kirsch, V., Brandt, T., Dieterich, M. Different EEG brain activity in right and left-handers during visually induced self-motion perception. *Journal of Neurology*. **267** (1), 79-90 (2020).
99. Kelly, R., Mizelle, J. C., Wheaton, L. A. Distinctive laterality of neural networks supporting action understanding in left- and right-handed individuals: An EEG coherence study. *Neuropsychologia*. **75**, 20-29 (2015).
100. O'Hare, A. J., Atchley, R. A., Young, K. M. Central and divided visual field presentation of emotional images to measure hemispheric differences in motivated attention. *Journal of Visualized Experiments*. (129), e56257 (2017).
101. Beatty, J. Task-evoked pupillary responses, processing load, and the structure of processing resources. *Psychological Bulletin*, . **91** (2), 276-292 (1982).
102. Wainstein, G. et al. Pupil size tracks attentional performance in attention-deficit/hyperactivity disorder. *Scientific Reports*. **7** (1), 8228 (2017).
103. Drueke, B. et al. Neural correlates of positive and negative performance feedback in younger and older adults. *Behavioral and Brain Functions*. **11**, 17 (2015).

104. Lezak, M. D. The problem of assessing executive functions. *International Journal of Psychology*. **17** (1-4), 281-297 (1982).
105. Oosterman, J. M., Wijers, M., Kessels, R. P. C. Planning or something else? Examining neuropsychological predictors of zoo map performance. *Applied Neuropsychology*. **20** (2), 103-109 (2013).
106. Keil, A., et al. Committee report: Publication guidelines and recommendations for studies using electroencephalography and magnetoencephalography. *Psychophysiology*. **51** (1), 1-21 (2014).
107. Abokyi, S., Owusu-Mensah, J., Osei, K. A. Caffeine intake is associated with pupil dilation and enhanced accommodation. *Eye*. **31** (4), 615-619 (2017).
108. Wilhelm, B., Stuibler, G., Lüdtke, H., Wilhelm, H. The effect of caffeine on spontaneous pupillary oscillations. *Ophthalmic & Physiological Optics*. **34** (1), 73-81 (2014).
109. McGinley, M. J., David, S. V., McCormick, D. A. Cortical membrane potential signature of optimal states for sensory signal detection. *Neuron*. **87** (1), 179-192 (2015).
110. Slotnick S. D. High density event-related potential data acquisition in cognitive neuroscience. *Journal of Visualized Experiments*. (38), e1945 (2010).
111. Lamm, C., Windischberger, C., Leodolter, U., Moser, E., Bauer, H. Co-registration of EEG and MRI data using matching of spline interpolated and MRI-segmented reconstructions of the scalp surface. *Brain Topography*. **14** (2), 93-100 (2001).
112. Schwartz, D. et al. Registration of MEG/EEG data with 3D MRI: Methodology and precision issues. *Brain Topography*. **9**, 101-116 (1996).
113. Laeng, B., Sirois, S., Gredebäck, G. Pupillometry: A window to the preconscious? Perspectives on psychological science. *Journal of the Association for Psychological Science*. **7** (1), 18-27 (2012).
114. Vandierendonck, A. A comparison of methods to combine speed and accuracy measures of performance: A rejoinder on the binning procedure. *Behavior Research Methods*. **49** (2), 653-673 (2017).
115. Vandierendonck, A. Further tests of the utility of integrated speed-accuracy measures in task switching. *Journal of Cognition*. **1** (1), 8 (2018).
116. Levene, H. Robust tests for equality of variances. In *Contributions to Probability and Statistics: Essays in Honor of Harold Hotelling.*, edited by Olkin, I., 278-292. Stanford University Press. Redwood City, CA (1960).
117. Zimmerman D. W. A note on preliminary tests of equality of variances. *The British Journal of Mathematical and Statistical Psychology*. **57** (Pt 1), 173-181 (2004).
118. D'Agostino, R. B., Belanger, A., D'Agostino, R. B. A suggestion for using powerful and informative tests of normality. *The American Statistician*. **44** (4), 316 (1990).
119. Shapiro S. S., Wilk, M. B. An analysis of variance test for normality (complete samples). *Biometrika*. **52** (3-4), 591-611 (1965).
120. Wilcoxon, F. Individual comparisons by ranking methods. *Biometrics Bulletin*. **1** (6), 80 (1945).
121. Fay, M. P., Proschan, M. A. Wilcoxon-Mann-Whitney or t-test? On assumptions for hypothesis tests and multiple interpretations of decision rules. *Statistics Surveys*. **4**, 1-39 (2010).
122. Delorme, A., Makeig, S. EEGLAB: An open-source toolbox for analysis of single-trial EEG dynamics

- including independent component analysis. *Journal of Neuroscience Methods*. **134** (1), 9-21 (2004).
123. Dimigen, O., Sommer, W., Hohlfeld, A., Jacobs, A. M., Kliegl, R. Coregistration of eye movements and EEG in natural reading: Analyses and review. *Journal of Experimental Psychology*. **140** (4), 552-572 (2011).
124. Mognon, A., Jovicich, J., Bruzzone, L., Buiatti, M. ADJUST: An automatic EEG artifact detector based on the joint use of spatial and temporal features. *Psychophysiology*. **48** (2), 229-240 (2011).
125. Bell, A. J., Sejnowski, T. J. A non-linear information maximization algorithm that performs blind separation. In *Advances in Neural Information Processing Systems 7.*, edited by Leen, T. K., Tesauro, G., Touretzky, D. S. MIT Press. Cambridge, MA (1995).
126. Plöchl, M., Ossandón, J. P., König, P. Combining EEG and eye tracking: Identification, characterization, and correction of eye movement artifacts in electroencephalographic data. *Frontiers in Human Neuroscience*. **6**, 278 (2012).
127. Pion-Tonachini, L., Kreutz-Delgado, K., Makeig, S. ICLabel: An automated electroencephalographic independent component classifier, dataset, and website. *NeuroImage*. **198**, 181-197 (2019).
128. Gartner, M., Grimm, S., Bajbouj, M. Frontal midline theta oscillations during mental arithmetic: Effects of stress. *Frontiers in Behavioral Neuroscience*. **9**, 96 (2015).
129. Wang, W., Viswanathan, S., Lee, T., Grafton, S. T. Coupling between theta oscillations and cognitive control network during cross-modal visual and auditory attention: Supramodal vs modality-specific mechanisms. *PLoS One*. **11** (7), e0158465 (2016).
130. Maris, E., Oostenveld, R. Nonparametric statistical testing of EEG- and MEG-data. *Journal of Neuroscience Methods*. **164** (1), 177-190 (2007).
131. Tadel, F., Baillet, S., Mosher, J. C., Pantazis, D., Leahy, R. M. Brainstorm: A user-friendly application for MEG/EEG analysis. *Computational Intelligence and Neuroscience*. **2011**, 879716 (2011).
132. Pascual-Marqui, R. D. Standardized low-resolution brain electromagnetic tomography (sLORETA): Technical details. *Methods and Findings in Experimental and Clinical Pharmacology*. **24** (Suppl D), 5-12 (2002).
133. Gramfort, A., Papadopoulos, T., Olivi, E., Clerc, M. OpenMEEG: Opensource software for quasistatic bioelectromagnetics. *Biomedical Engineering Online*. **9**, 45 (2010).
134. Destrieux, C., Fischl, B., Dale, A., Halgren, E. Automatic parcellation of human cortical gyri and sulci using standard anatomical nomenclature. *NeuroImage*. **53** (1), 1-15 (2010).
135. Orr, J. M., Weissman, D. H. Anterior cingulate cortex makes 2 contributions to minimizing distraction. *Cerebral Cortex*. **9** (3), 703-711 (2009).
136. Christoff, K., Gabrieli, J. D. E. The frontopolar cortex and human cognition: Evidence for a rostrocaudal hierarchical organization within the human prefrontal cortex. *Psychobiology*. **28** (2), 168-186 (2000).
137. Nitschke, K., Köstering, L., Finkel, L., Weiller, C., Kaller, C. P. A meta-analysis on the neural basis of planning: Activation likelihood estimation of functional brain imaging results in the Tower of London task. *Human Brain Mapping*. **38** (1), 396-413 (2017).

138. Barbey, A. K., Koenigs, M., Grafman, J. Dorsolateral prefrontal contributions to human working memory. *Cortex*. **49** (5), 1195-1205 (2013).
139. Le Van Quyen, M. et al. Comparison of Hilbert transform and wavelet methods for the analysis of neuronal synchrony. *Journal of Neuroscience Methods*. **111** (2), 83-98 (2001).
140. Bokil, H., Andrews, P., Kulkarni, J. E., Mehta, S., Mitra, P. P. Chronux: A platform for analyzing neural signals. *Journal of Neuroscience Methods*. **192** (1), 146-151 (2010).
141. Sato, N., Yamaguchi, Y. EEG theta regulates eye saccade generation during human object-place memory encoding. In *Advances in Cognitive Neurodynamics ICCN 2007.*, 429-434. Springer. Dordrecht, the Netherlands (2008).
142. Zaki, J., Ochsner, K. The need for a cognitive neuroscience of naturalistic social cognition. *Annals of the New York Academy of Sciences*. **1167**, 16-30 (2009).
143. Shamay-Tsoory, S. G., Mendelsohn, A. Real-life neuroscience: An ecological approach to brain and behavior research. *Perspectives on Psychological Science*. **14** (5), 841-859 (2019).
144. Diamond, A. Executive functions. *Annual Review of Psychology*. **64**, 135-168 (2013).
145. Dudai, Y. *Memory from A to Z: Keywords, Concepts and Beyond*. Oxford University Press. New York, NY (2002).
146. Kingstone, A., Smilek, D., Ristic, J., Friesen, C. K., Eastwood, J. D. Attention, researchers! It is time to take a look at the real world. *Current Directions in Psychological Science*. **12** (5), 176-180 (2003).
147. Morris, R. G., Ward, G. Introduction to the psychology of planning. In *The Cognitive Psychology of Planning.*, edited by Morris, R., Ward, G. Psychology Press. Hove, UK (2005).
148. Zwosta, K., Ruge, H., Wolfensteller, U. Neural mechanisms of goal-directed behavior: Outcome-based response selection is associated with increased functional coupling of the angular gyrus. *Frontiers in Human Neuroscience*. **9**, 180 (2015).
149. Owen, A. M., Doyon, J., Petrides, M., Evans, A. C. Planning and spatial working memory: A positron emission tomography study in humans. *European Journal of Neuroscience*. **8** (2), 353-364 (1996).
150. Ossandon, T. et al. Efficient "pop-out" visual search elicits sustained broadband gamma activity in the dorsal attention network. *Journal of Neuroscience*. **32** (10), 3414-3421 (2012).
151. Lezak, M. D. *Neuropsychological Assessment.*, 3rd edition. Oxford University Press. New York, NY (1995).
152. Lin, H., Saunders, B., Hutcherson, C. A., Inzlicht, M. Midfrontal theta and pupil dilation parametrically track subjective conflict (but also surprise) during intertemporal choice. *NeuroImage*. **172**, 838-852 (2018).
153. Yu, S., Mückschel, M., Beste, C. Superior frontal regions reflect the dynamics of task engagement and theta band-related control processes in time-on task effects. *Scientific Reports*. **12** (1), 846 (2022).
154. Nakatani, H., van Leeuwen, C. Antecedent occipital alpha band activity predicts the impact of oculomotor events in perceptual switching. *Frontiers in Systems Neuroscience*. **7**, 19 (2013).

155. Velasques, B. et al. Changes in saccadic eye movement (SEM) and quantitative EEG parameter in bipolar patients. *Journal of Affective Disorders*. **145** (3), 378-385 (2013).
156. Bodala, I. P., Li, J., Thakor, N. V., Al-Nashash, H. EEG and eye tracking demonstrate vigilance enhancement with challenge integration. *Frontiers in Human Neuroscience*. **10**, 273 (2016).
157. Dimigen O. Optimizing the ICA-based removal of ocular EEG artifacts from free viewing experiments. *NeuroImage*. **207**, 116117 (2020).